

University of Windsor

Scholarship at UWindor

Electronic Theses and Dissertations

Theses, Dissertations, and Major Papers

2011

Impact of Cable-deck Interaction on the Efficiency of External Damper in Controlling Stay Cable Vibration on Cable-Stayed Bridges

Krishanth Korallalage
University of Windsor

Follow this and additional works at: <https://scholar.uwindsor.ca/etd>

Recommended Citation

Korallalage, Krishanth, "Impact of Cable-deck Interaction on the Efficiency of External Damper in Controlling Stay Cable Vibration on Cable-Stayed Bridges" (2011). *Electronic Theses and Dissertations*. 81.

<https://scholar.uwindsor.ca/etd/81>

This online database contains the full-text of PhD dissertations and Masters' theses of University of Windsor students from 1954 forward. These documents are made available for personal study and research purposes only, in accordance with the Canadian Copyright Act and the Creative Commons license—CC BY-NC-ND (Attribution, Non-Commercial, No Derivative Works). Under this license, works must always be attributed to the copyright holder (original author), cannot be used for any commercial purposes, and may not be altered. Any other use would require the permission of the copyright holder. Students may inquire about withdrawing their dissertation and/or thesis from this database. For additional inquiries, please contact the repository administrator via email (scholarship@uwindsor.ca) or by telephone at 519-253-3000ext. 3208.

Impact of Cable-deck Interaction on the Efficiency of External Damper in Controlling Stay Cable Vibration on Cable-Stayed Bridges

By

Krishanth Koralalage

A Thesis

Submitted to the Faculty of Graduate Studies Through Civil and Environmental Engineering

in Partial Fulfillment of the Requirements for the Degree of Master of Applied Science at the

University of Windsor

Windsor, Ontario, Canada

2011

© 2011 Krishanth Koralalage

Impact of Cable-deck Interaction on the Efficiency of External Damper in
Controlling Stay Cable Vibration on Cable-Stayed Bridges

By

Krishanth Koralalage

APPROVED BY:

Dr. D. Green, Outside Department Reader
Department of Mechanical, Automotive and Material Engineering

Dr. F. Ghrib, Department Reader
Department of Civil and Environmental Engineering

Dr. S. Cheng, Advisor
Department of Civil and Environmental Engineering

Dr. T. Bollisetti, Chair of Defense
Department of Civil and Environmental Engineering

11 April 2011

DECLARATION OF ORIGINALITY

I hereby certify that I am the sole author of this thesis and that no part of this thesis has been published or submitted for publication.

I certify that, to the best of my knowledge, my thesis does not infringe upon anyone's copyright nor violate any proprietary rights and that any ideas, techniques, quotations, or any other material from the work of other people included in my thesis, published or otherwise, are fully acknowledged in accordance with the standard referencing practices. Furthermore, to the extent that I have included copyrighted material that surpasses the bounds of fair dealing within the meaning of the Canada Copyright Act, I certify that I have obtained a written permission from the copyright owner(s) to include such material(s) in my thesis and have included copies of such copyright clearances to my appendix.

I declare that this is a true copy of my thesis, including any final revisions, as approved by my thesis committee and the Graduate Studies office, and that this thesis has not been submitted for a higher degree to any other University or Institution.

ABSTRACT

External dampers are widely used to control vibrations of stay cables on cable-stayed bridges. In general, the estimation of the damping of a stay cable in a cable-damper system is done based on the assumption that the bridge stay cable has fixed supports at both ends and the damper has a fixed support on the deck. But long-span bridges experience frequent bridge-girder vibrations under dynamic loadings due to long span length, light weight and flexible nature. Therefore, the assumptions of fixed support for the cable and damper is no longer valid in the case of long-span bridges.

An analytical model has been proposed in the current study to determine the damping property of a bridge stay cable when attached with a damper, by considering the effect of bridge-deck vibration on the cable and the damper. The static and the dynamic behaviour of the cable-damper-deck system have been simulated in the model. The validity of the model was verified by assuming a very rigid equivalent beam and was compared with the results obtained from a cable fixed end case. A Matlab program was developed to perform matrix calculations and iterations associated with the model. Associated dynamic analysis was carried out using the finite element model in ABAQUS 6.9.

Case studies were conducted to investigate the effect of cable-deck interaction on the damper efficiency for cable-stayed bridges with different span lengths. The range of main span length that requires the consideration of bridge-deck vibration for the estimation of damper efficiency was proposed.

ACKNOWLEDGEMENTS

I would like to express my deep gratitude to my supervisor Dr. Shaohong Cheng for this dissertation. Her lectures have laid a sound foundation for the work and her constant support and guidance throughout the project is greatly appreciated.

Also I would like to thank Dr. Fouzi Ghrib for his valuable advice on my project and for his lectures which have enlightened me with conceptual background in structural engineering. The advice and support of Dr. Bollisetti in my learning process is also thankfully acknowledged.

The comments of Dr. Green and the help of the laboratory staff and non-technical staff of the Civil Engineering Department are also gratefully acknowledged.

Finally and most importantly, I would like to thank my wife, Chandrika and my two children, Thewmi and Sithumi, who always helped me in many ways for successful completion of my thesis.

TABLE OF CONTENTS

DECLARATION OF ORIGINALITY	iii
ABSTRACT.....	iv
ACKNOWLEDGEMENTS.....	v
LIST OF TABLES.....	ix
LIST OF FIGURES	x
NOMENCLATURE.....	xii

CHAPTER

I. INTRODUCTION

1.1 Background	1
1.2 Motivations	4
1.3 Objectives.....	6

II. REVIEW OF LITERATURE

2.1 Free vibration of a suspended uniform cable	8
2.2 Free vibration of a suspended cable attached to a transverse linear viscous damper.....	17
2.3 Free vibration of multi-span continuous uniform beams	22
2.4 Effect of cable-deck interaction on vibration of a damped stay cable	23

**III. ANALYTICAL FORMULATION OF A CABLE -DAMPER-DECK
COUPLED SYSTEM**

3.1 Free in-plane vibration of an inclined taut cable.....26

3.2 Free vibration analysis of a three-span continuous beam..... 34

3.3 Equation of motion of cable-damper -deck coupled system.....41

3.4 Solution to equation of motion.....56

IV. CASE STUDY

4.1 Description of the example bridge60

4.2 Effectiveness of damper by considering the cable-deck
interaction.....63

4.3 Comparison with existing models67

4.4 Case studies..... 70

V. CONCLUSIONS AND RECOMMENDATIONS

Concluding remarks.....80

Recommandations for future research82

APPENDICES

Appendix A: Relationship of m_2 and EI in the equivalent beam
based on the static condition83

Appendix B: Relationship of m_2 and EI in the equivalent beam
based on the first vertical bending frequency of the

bridge.....	89
Appendix C: Derivation of modal damping ratio of an inclined taut string with fixed supports attached to a linear viscous damper.....	91
Appendix D: Matlab program for matrix calculation and iterations..	95
Appendix D: Input source code for ABAQUS simulation.	98
REFERENCES.....	102
VITA AUCTORIS	109

LIST OF TABLES

Table 4-1	The main parameters of the longest cable and damper	64
Table 4-2	Input parameters in matrix G	66
Table 4-3	Summary of results	69
Table 4-4	Summary of bridge data	76
Table 4-5	Summary of equivalent beam data	77
Table 4-6	Summary of case study results	78

LIST OF FIGURES

Figure 2-1	Definition diagram for cable vibration	09
Figure 2-2	Static profile of an inclined cable Irvine (1980)	12
Figure 2-3	Geometry of an inclined cable Wu et al (2005)	13
Figure 2-4	Displacement of an element of the cable in the local coordinate system Wu et al (2005)	15
Figure 2-5	Taut cable with external viscous damper	17
Figure 2-6	Layout of a cable-damper system	20
Figure 2-7	An element of a uniform beam subjected to vibration	22
Figure 2-8	Simplified theoretical model of cable-deck-damper system Liang et al (2008)	25
Figure 3-1	Static forces acting on an element of an inclined cable	27
Figure 3-2	Schematic diagram of a three-span continuous beam	34
Figure 3-3	Schematic diagram of the three-span continuous bridge	40
Figure 3-4	Graph of $\det[G]$ vs λ	40
Figure 3-5	Schematic diagram of the theoretical model of cable-deck-damper system	42
Figure 4-1	Sutong bridge- Jiangsu province, China	62
Figure 4-2	Schematic diagram of span arrangements with only outermost cables in Sutong bridge	62
Figure 4-3	A viscous damper attached to a bridge stay cable	63
Figure 4-4	Cable-damper-deck coupled system for the longest cable in Sutong bridge	64

Figure 4-5	Simplified cantilever beam model used by Liang et al (2008)	68
Figure 4-6	View of the Stonecutters Bridge at the entrance to the Kwai Chung container port	71
Figure 4-7	Tatara Bridge	72
Figure 4-8	Third Nanjing Yangtze Bridge	73
Figure 4-9	Donghai Bridge	74
Figure 4-10	Graph of damping ratio vs main span length	78
FigureA-1	Three-span continuous beam under self weight, including bending moment diagram for each span in simply supported case	84
Figure A-2	Three-span continuous beam subjected to a concentrated load, including bending moment diagram for simply supported case.	86
Figure B-1	Schematic diagram of the numerical model of cable-deck system	89
Figure C-1	A cable-damper system	91

NOMENCLATURE

A_1, A_2, A_3, A_4, A_5	coefficients of bridge girder displacement functions
a	horizontal distance from the pylon to the cable-damper connecting point.
a'	horizontal distance from the cable anchorage to the cable-damper connecting point.
B_1, B_2, B_3, B_4, B_5	coefficients of bridge girder displacement functions
b	horizontal distance from pylon to the damper-deck connecting point.
b'	horizontal distance from the cable anchorage to the damper-deck connecting point.
C_0	coefficient of damper
C_1, C_2, C_3, C_4, C_5	coefficients of bridge girder displacement functions
D_1, D_2, D_3, D_4, D_5	coefficients of bridge girder displacement functions
E	elastic modulus of bridge girder
EI	flexural rigidity of bridge girder
f_c	1 st modal vibration frequency of stay cable
f_s	1 st vertical bending frequency of bridge girder

F_u	horizontal damping force on cable
F_v	vertical damping force on cable
F_w	vertical damping force on bridge girder
H	horizontal component of cable tension
L	horizontal distance from left pylon to cable anchorage point
L_1, L_2, L_3	span lengths of bridge girder
L_4	horizontal distance from right pylon to cable anchorage point
m_1	mass density of cable
m_2	equivalent mass density of bridge girder
P_1, P_2	coefficients of cable displacement functions
Q_1, Q_2	coefficients of cable displacement functions
T	cable tension under static condition
u	horizontal displacement function of cable $u(x, t)$
u_{DG}	horizontal displacement function of cable in span DG
u_{HG}	horizontal displacement function of cable in span HG

v	vertical displacement function of cable $v(x, t)$
v_{DG}	vertical displacement function of cable in span DG
v_{HG}	vertical displacement function of cable in span HG
w	vertical displacement function of cable $w(x, t)$
w_{AB}	vertical displacement function of bridge girder in span AB
w_{BC}	vertical displacement function of bridge girder in span BC
w_{CD}	vertical displacement function of bridge girder in span CD
w_{ED}	vertical displacement function of bridge girder in span ED
w_{FE}	vertical displacement function of bridge girder in span FE
x	horizontal distance measured from the left pylon
x_1, x_2, x_3, x_4, x_5	horizontal displacements measured along the bridge girder as indicated
x_c	horizontal distance measured from the left pylon in span HG
x'_c	horizontal distance measured from the cable anchorage point in span DG

y	downward vertical displacement of the static cable profile measured from the pylon-cable anchorage point
β	$\beta = \frac{C_0 \omega}{\gamma T \cos \theta}$
δ	Dirac delta function
θ	angle of inclination of the cable to the horizontal axis
ω	frequency of vibration of the entire system
η	$\eta = C_0 \omega / (\lambda^3 EI)$
λ	$\lambda = \sqrt[4]{\omega^2 m_2 / EI}$
γ	$\gamma = \frac{\omega}{T \cos \theta} \sqrt{\frac{m_1}{T}}$

CHAPTER I INTRODUCTION

1.1 Background

One main achievement of the recent advancement in bridge engineering is the use of much longer spans of girders in cable-stayed bridges and thereby efficient use of materials and other resources in construction and maintenance. Light weight of the structural components and use of longer spans results in more slender elements which are susceptible for vibration under dynamic excitations. The cables in long-span cable-stayed bridges are prone to exhibit high amplitude of oscillation due to their light mass, high flexibility and very low intrinsic damping. It has become more important and serious matter of concern in recent years due to the rapid development of long-span cable-stayed bridges and due to the incidence of high amplitude cable vibration observed on bridge site and experimental studies in the past few decades.

The complex behavior of cable-stayed bridges when subjected to dynamic loads, such as wind, traffic or seismic excitation is a long standing issue in bridge engineering. The non linear interaction between local cable vibrations and bridge deck vibrations is an issue which can lead to very large cable vibrations or high amplitudes of deck vibrations. These can in turn lead to an issue of structural safety, user discomfort or fatigue damage. Wind-induced cable vibrations are identified as the most common in bridge stay cables. The initiative and the amplitude of excitation depend on the flow characteristics of wind, the geometry and the dynamic properties of the cable. Depending on their mechanisms, wind-induced cable vibration mostly related to stay cables can be categorized as following types (Cheng & Tanaka, 2002): a) Vortex-induced vibration; b) Buffeting; c)

Wake galloping; d) Rain-wind-induced vibration; e) High-speed vortex excitation; f) Dry inclined cable galloping.

Vortex-shedding is a phenomenon that excites cables under flow of wind. If the natural frequency of the cable lies in close proximity of the shedding frequency of vortices form in the wake of the cable, vortex resonance would occur resulting high amplitude cable vibration. The frequency of vortex shedding is much higher for normal wind speeds than the range of natural frequency of bridge stay cables to excite in first few modes. Therefore it is unlikely that vortex shedding be critical in bridge stay cable excitation (Strouhal, 1898).

Buffeting is a vibration forced by the velocity fluctuation of the oncoming flow and it is directly related to the level of wind speed. Buffeting has not been found to cause serious effect on bridge stay cable vibration. However, this frequent low amplitude vibration could induce fatigue damage and thus threats safety of the bridge.

Based on field observations and measurements, it was found (Hikami & Shiraishi, 1988; Matsumoto et al, 1989b; Yoshimura et al, 1989; Main et al, 1999; 2001) that rain-wind induced vibration usually occurs at wind speeds of 6-18 m/s, accompanied with light rain. Wind is in a direction 20° - 60° skewed to the cable plane with low turbulence intensity. The majority of the cables that experienced this vibration, locate in the leeward side of the bridge pylon and are geometrically declined in the mean wind direction. The formation of upper water rivulet on the cable surface seems to be a key factor (Yamada et al, 1997). This phenomenon is very common in bridge stay cables.

High speed vortex excitation has been observed in field and in wind tunnel tests without precipitation. It occurs at much higher wind velocity ranges than that for regular

vortex-induced vibration. Some studies (Matsumoto et al, 1990) suggest that this phenomenon could be caused by regular Karmen vortex shedding and axial vortex shedding along the cable axis.

Dry inclined cable galloping is an excitation phenomena identified during wind tunnel testing (Cheng & Tanaka, 2002). Although it has not yet been observed on site, , it causes a big concern in the bridge industry due to its divergent nature and uncertain onset conditions. One of the possible mechanisms is proposed to be linked to negative aerodynamic damping (Cheng & Tanaka, 2002). Research about this phenomenon is still under way.

Suppressing the vibration of bridge stay cables is of prime importance since the effect of vibration of stay-cable as a key structural element, is directly related to the serviceability and life span of the entire bridge. Frequent vibrations could lead to connection failures, breakdown of the corrosion protection system, and fatigue failure of the cable itself. On the other hand, excessive vibration will be a safety issue for the entire structure, and may result in sudden cable failure leaving the bridge unusable. Therefore, different counter measures are adopted to control the cable vibration. They can be categorized mainly into two types, aerodynamic and mechanical types.

In aerodynamic methods, the surface of the bridge stay cable is modified to ensure that rain-wind related excitations are minimized . Some of the surface treatments adopted at present are dimpled surface on Tatara bridge in Japan, (Verlogeux, 1998); helical wire whirling surface on Vasco da Gama bridge in Portugal (Bosdogianni & Olivari, 1996) and axially protuberant surface cables on Higashi-Kobe bridge in Japan (Saito et al, 1994). Mechanical improvements are directed to dissipate kinetic energy of

the cable by using external dampers near anchorage points and dissipate kinetic energy and improve stiffness by connecting adjacent cables together using cable cross-ties. Transverse elements as cross-ties in the cable plane will effectively reduce the length of the cross cable, thereby increasing the frequency and the stiffness of the system. Also the cross-ties will act as a means of transferring energy from the excited cable to stiffer elements (Yamaguchi & Nagahawatta, 1995). Use of external dampers at or near the cable anchorage point is much more popular than use of cross-ties since it does not interfere with the aesthetical appearance of the bridge. External dampers can be classified as passive, semi-active and active. All three types exert a transverse damping force on the cable based on the velocity at the contact point. Damper force induced by the passive damper will have a predefined relation with the velocity at the contact point whereas semi-active and active dampers exerts optimum damper force based on the amount of vibration present and have a nonlinear force variation.

1.2 Motivations

External dampers have been used as a measure of controlling transverse cable vibration mostly induced by dynamic excitation such as wind. The behaviour of a stay cable when attached to a transverse damper has been studied by many researchers (Kovacs, 1982; Yoneda & Maeda, 1989; Uno et al, 1991 and Pacheco et al, 1993). The approximate relations between damper size, maximum achievable damping ratio and damper installation location have been developed for design purposes by treating the cable as a taut string. Subsequently, the above relationships were further developed by incorporating cable parameters, bending stiffness and sag extensibility (Tabatabai and

Mehrabi,1998). The experimental and analytical findings (Tabatabai & Mehrabi, 2000) confirmed that higher damper size do not necessarily result in higher cable damping ratios. By formulating simplified equations and damping estimation curves using the non-linear properties of cable, properties of damper and damper location, Tabatabai & Mehrabi (1998) introduced a design tool for damper design.

It is noted that all the existing studies are based on the underlying assumption that the bridge deck does not move and the supports of the cable and the damper at the deck level are fixed. Although this assumption could be accepted for a short-span bridge which has relatively rigid super structure, it may not be applicable for more flexible medium to long-span bridges. In a real bridge configurations, the two ends of an inclined cable are connected with pylon and deck respectively. This does not comply with the fixed-fixed support conditions assumed in the existing studies. Especially for longer span cable-stayed bridges, the bridge girders are light weight and less rigid. The bridge deck which provides the support for one end of the cable and support for the damper thus should be treated as moving supports for accurate prediction of the damper efficiency. The force exerted by the viscous damper on the cable is proportional to the relative velocity of the cable at the contact point of the damper, and this relative velocity could only be accurately predicted if the bridge girder vibration is taken into account in the analysis. Therefore, the focus of this thesis is to incorporate the cable-deck interaction in the dynamic analysis of a damped stay cable vibration to predict more accurately the damping effects of the damper.

1.3 Objectives

The objectives of the current study are summarized as follows.

1. Propose an analytical model of cable-deck-damper system to investigate cable-deck interaction on damper performance.
2. Develop a method to analyze the dynamic behavior of the cable-deck–damper system.
3. Investigate the influence of cable-deck interaction on the damper efficiency.
4. Conduct case studies to compare the results from the proposed model with those from the existing methods.
5. Perform parametric studies to establish the range of bridge span length that requires the consideration of cable-deck interaction in external damper design.
6. Shed light on the development of more accurate optimum damper design for longer span cable-stayed bridges.

To achieve the above objectives, the scope of the current study thus includes

- Free vibration analysis of horizontal and inclined cables by considering the effects of sag and cable bending stiffness.
- Free vibration analysis of uniform beams with multiple spans and different end conditions.
- Dynamic analysis of a cable-damper system by considering the effects of cable sag extensibility, bending stiffness, damper properties and damper location.
- Development of an analytical model of cable-deck-damper system to analyze the motion and evaluate the effect of cable-deck interaction on damper efficiency.

- Conduct case studies.
- Perform a parametric study to establish the range of bridge span length for which the developed model should be used to evaluate damper performance.

CHAPTER II REVIEW OF LITERATURE

A brief review of the literature in cable dynamics and free vibration of multi-span continuous beams which relates to the current work is presented in this chapter.

2.1 Free vibration of a suspended uniform cable.

2.1.1 Horizontal Cable

A linear theory for the free vibrations of horizontally suspended uniform cables was presented by Irvine & Caughey (1974), where the ratio of sag to span is about 1:8 or less. It is assumed that the static effects of cable elasticity govern the horizontal tension and the sag of the cable. A diagram of a horizontally suspended cable which indicates the parameters of subsequent equations is shown in Fig. 2-1. In the diagram, u is the longitudinal component and v is the vertical component of in-plane motion, w is the transverse horizontal component (perpendicular to the vertical plane through supports) of motion, l is the length of the span and d is the maximum static deflection observed at mid-span. x and y represent the coordinates of the static profile of the cable as shown. The transverse horizontal motion, as the easily excited mode, is uncoupled from the in-plane motion to the first order since there is no involvement of cable tension. In the in-plane mode, the amplitude of the corresponding longitudinal modal component is always substantially less than the amplitude of the vertical motion. Since the sag of the cable is considered to be small, the longitudinal component of the motion has been neglected in the analysis.

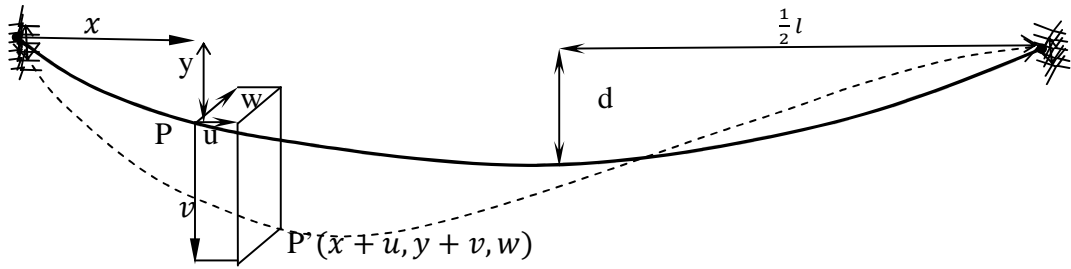


Figure 2-1 Definition diagram for cable vibration

The transverse horizontal modal frequencies are obtained as the solution to an eigenvalue problem of

$$H \frac{d^2 \tilde{w}(x)}{dx^2} + m\omega^2 \tilde{w}(x) = 0 \quad (2-1)$$

where $w(x, t) = \tilde{w}(x)e^{i\omega t}$ is the transverse component of motion, H is the horizontal component of cable tension and m is the mass density of the cable. The circular frequency of the transverse vibration is given by $\omega_n = n\pi/l\sqrt{H/m}$, $n = 1, 2, 3, \dots$, where l is the length of the cable and n is the mode number.

The equation of in-plane vertical motion is given by

$$H \frac{\partial^2 v}{\partial x^2} + h \frac{d^2 y}{dx^2} = m \frac{\partial^2 v}{\partial t^2} \quad (2-2)$$

where h is the additional horizontal component of cable tension due to cable vibration.

The elastic and geometric compatibility of the cable element is given by Irvine (1980).

$$h \frac{(ds/dx)^3}{E_c A_c} = \frac{\partial u}{\partial x} + \frac{dy}{dx} \frac{\delta v}{\delta x} \quad .(2-3)$$

where A_c is the cross sectional area of the cable, E_c is the elastic modulus of the cable and ds is the length of the cable element considered.

The in-plane vertical motion is considered as two fold for computational simplicity, that is symmetric mode and anti-symmetric mode. Frequency for anti-symmetric in-plane motion of which no additional cable tension is developed is obtained from Eq.(2-2) as $\omega_n = \frac{2n\pi}{l} \sqrt{\frac{H}{m}}$ where $n = 1, 2, 3, \dots$ is the mode number. The anti-symmetric vertical modal component is given by

$$v_n(x) = A_n \sin\left(\frac{2n\pi x}{l}\right), n = 1, 2, 3, \dots \quad (2-4)$$

The longitudinal component of the anti-symmetric model motion can be found when the additional tension in Eq.(2-3) is zero. It leads to

$$u_n(x) = -4\left(\frac{d}{l}\right)A_n \left\{ \left(1 - 2\left(\frac{x}{l}\right)\right) \sin\left(\frac{2n\pi x}{l}\right) + \frac{1}{n\pi} \left(1 - \cos\left(\frac{2n\pi x}{l}\right)\right) \right\} \quad (2-5)$$

where A_n is the amplitude of the anti-symmetric vertical component of the n^{th} mode. It is clear from the above expression that when the cable becomes flatter, the amplitude of the longitudinal component becomes smaller.

In the case of the symmetric in-plane modes, the additional cable tension is non-zero. It is treated as a function of time alone. The solution to the eigenvalue problem

leads to the following transcendental equation, from which the natural frequencies of the symmetric in-plane modes may be found (Irvine & Caughy, 1974).

$$\tan\left(\frac{1}{2}\beta l\right) = \left(\frac{1}{2}\beta l\right) - \left(\frac{4}{\lambda^2}\right)\left(\frac{1}{2}\beta l\right)^3 \quad (2-6)$$

where $\lambda^2 = \left(\frac{8d}{l}\right)^2 \frac{l}{HL_e/E_c A_c}$ is called the Irvine parameter and $L_e = \int_0^l (ds/dx)^3 dx \cong l(1+8dl/2)$ is the elastic compatibility condition of the cable. The Irvine parameter describes the relation between cable geometry and elasticity. It governs natural frequencies and mode shapes of the cable motion. For example, if λ^2 is very large, i.e. if the cable is theoretically inextensible, the above transcendental equation becomes $\tan\left(\frac{1}{2}\beta l\right) = \left(\frac{1}{2}\beta l\right)$. This relationship is found in other problems of mechanics, i.e. torsional and flexural buckling of struts under certain boundary conditions. In the present study, the cable is idealized as a taut string, i.e. EI and sag are ignored in the formulation. The value of λ^2 represents taut string is zero. Equation (2-6) thus becomes $\tan\left(\frac{1}{2}\beta l\right) = -\infty$ and the first root will be $\beta l = \pi$ which is used in the analysis.

2.1.2 Inclined Cable

Formulations relevant to the motion of cables supported at the same level is of less use in the analysis of bridge stay cables since the cable arrangements are always inclined. A simplified solution to the static profile of an inclined cable shown in Fig. 2-2 is given by Irvine (1980).

$$Z = \frac{1}{2}X(1-X)\left\{1 + \frac{\varepsilon}{6}(1-2X)\right\}. \quad (2-7)$$

where Z, X and ε are the non-dimensional parameters defined as forms given by

$$Z = z/(mg \sec^2 \theta l^2 / H), \quad X = x/l \text{ and } \varepsilon = \frac{mgl \sin \theta}{H},$$

m is the mass density, l is the cable length, H is horizontal component of cable tension and θ is the angle of inclination

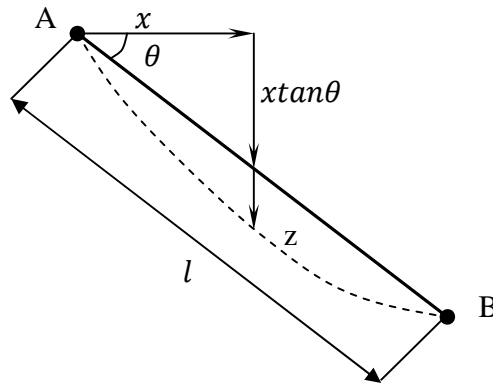


Figure 2- 2 Static profile of an inclined cable (Irvine ,1980)

of the cable with respect to the horizontal axis. The above derivation is done by neglecting the second order terms of the derivatives in the static equilibrium equation. A similar formulation was used (Wu et al ,2005) to obtain natural frequencies and mode shapes of an inclined cable as follows:

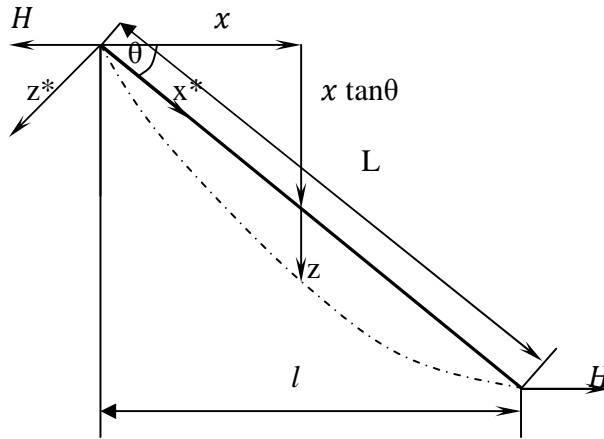


Figure 2-3 Geometry of an inclined cable (Wu et al, 2005)

The static profile of an inclined cable as shown in Fig. 2-3 is given by

$$\bar{z} = \frac{1}{2}\bar{x}(1 - \bar{x})\left\{1 + \frac{\varepsilon}{6}(1 - 2\bar{x})\right\} + O(\varepsilon^2) \quad (2-8)$$

Where the non dimensional parameters \bar{z} and \bar{x} are given by $\bar{z} = z/L$ and $\bar{x} = x/L$. Also $\bar{z} = \bar{z}/8\beta\cos\theta$, $\beta = mgL/8H\sec\theta$, and $\varepsilon = mgL/(H\sec\theta\sin\theta) = 8\beta\sin\theta$. By substituting $x = x^*\cos\theta - z^*\sin\theta$, $z = z^*/\cos\theta$ in Eq. (2-8), the profile can be obtained in the local coordinate system as

$$\bar{z}^* = \frac{1}{2}\bar{x}^*(1 - \bar{x}^*)\left\{1 - \frac{\varepsilon}{3}(1 - 2\bar{x}^*)\right\} + O(\varepsilon^2). \quad (2-9)$$

The equations of in-plane motion of an inclined cable in the local coordinate system are given by (Wu et al, 2005)

$$\frac{d}{ds}((T + \tau)\left(\frac{dx^*}{ds} + \frac{\partial u^*}{\partial s}\right)) = m \frac{\partial^2 u^*}{\partial t^2} - mg \sin \theta \quad (2-10)$$

$$\frac{d}{ds}((T + \tau)\left(\frac{dz^*}{ds} + \frac{\partial w^*}{\partial s}\right)) = m \frac{\partial^2 w^*}{\partial t^2} - mg \cos \theta \quad (2-11)$$

where τ is the additional tension generated, u^* is the in-plane longitudinal displacement in x^* direction and w^* is the transverse displacement in z^* direction. Displacement of an element of the cable in the local coordinate system is shown in Fig.2-4. Removing self-weight components from Eqs. (2-10) and (2-11) based on the cable static profile, the following equations of motion can be obtained in the local coordinate system.

$$\frac{d}{ds}\left(\tau \frac{dx^*}{ds} + (T + \tau) \frac{\partial u^*}{\partial s}\right) = m \frac{\partial^2 u^*}{\partial t^2} \quad (2-12)$$

$$\frac{d}{ds}\left(\tau \frac{dz^*}{ds} + (T + \tau) \frac{\partial w^*}{\partial s}\right) = m \frac{\partial^2 w^*}{\partial t^2}. \quad (2-13)$$

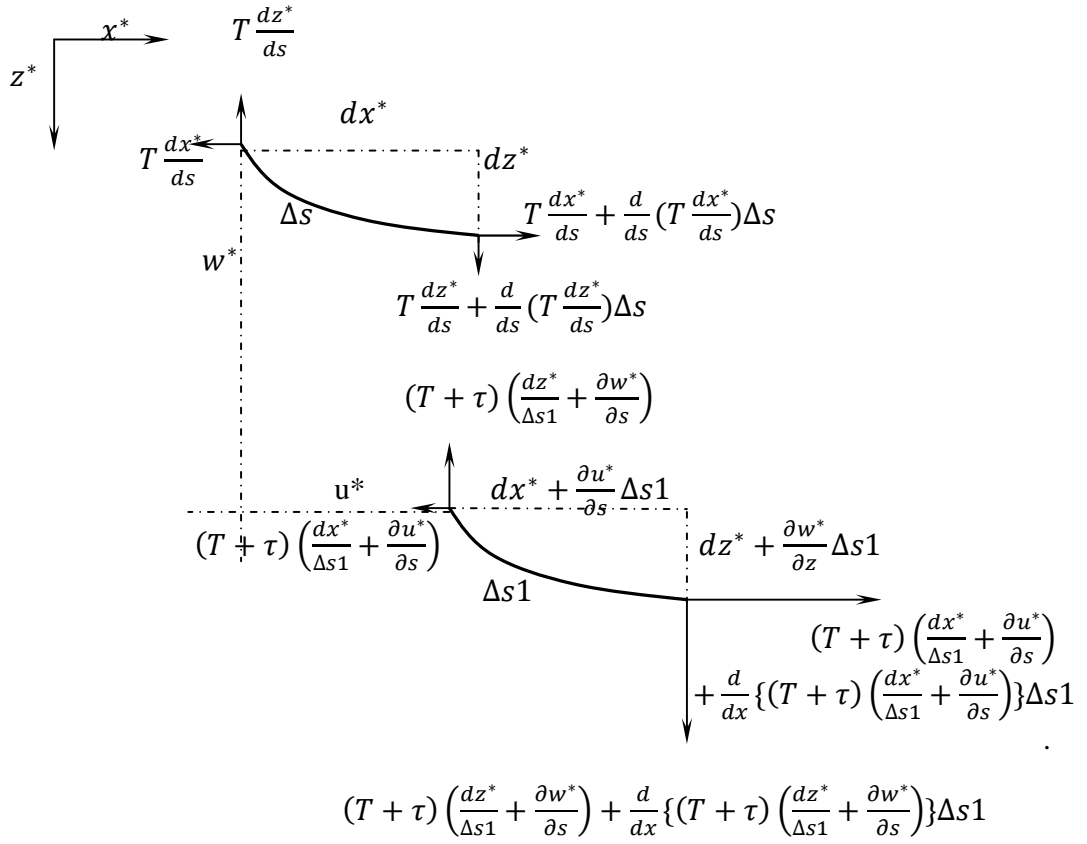


Figure 2-4 Displacement of an element of cable in the local coordinates(Wu et al, 2005)

If a flat sag cable is considered, the longitudinal motion can be neglected. By substituting $h^* = \tau \frac{dx^*}{ds}$ and $H^* = T \frac{dx^*}{ds}$ and assuming h^* is constant along the cable, $ds \approx dx^*$, Eq. (2-13) can be reduced to:

$$h^* \frac{d^2 z^*}{dx^{*2}} + (H^* + h^*) \frac{\partial^2 w^*}{\partial x^{*2}} = m \frac{\partial^2 w^*}{\partial t^2}. \quad (2-14)$$

Using Eq.(2-14) and the elastic compatibility of the cable, and adopting a method similar to that of Irvine & Caughey (1974) the following transcendental equation was obtained for the in-plane modal shapes and natural frequencies of an inclined cable (Wu et al, 2005).

$$\frac{4}{\lambda^2} \left(\frac{\pi\omega}{2}\right)^3 = \left(1 + \frac{\varepsilon^2}{3}\right) \frac{\pi\omega}{2} - \tan \frac{\pi\omega}{2} + \frac{\varepsilon^2}{\tan \pi\omega/2} - \frac{2\varepsilon^2}{\pi\omega} \quad (2-15)$$

where $\lambda^2 = \frac{k^2(8\beta\cos\theta)^2}{L_e}$ is the Irvine parameter and $k^2 = EA/(H\cos\theta)$.

Even though the static profile of an inclined cable considered in the current study is similar to that described by Wu et al (2005), the cable here is idealized as a taut string and its support at the deck level is no longer fixed.

A more accurate solution to the free vibrations of an extensible, sagging inclined cable was given by Triantafyllou (1983). He identified that the general asymptotic solution to the linear dynamic problem of a taut inclined cable had two physical mechanisms. The solution corresponded to the elastic waves changed from sinusoidal to exponential as the curvature increased. It occurred along the cable when the supports were at two different elevations. The part of the cable close to the higher support hung almost vertical. The part of the cable close to the lower support lied more flat. The motion of the nearly vertical part exhibited properties of an elastic chain, where as that of the nearly horizontal part exhibited properties of a taut wire. This phenomenon was accompanied by a shift of the natural frequency of the symmetric mode towards the natural frequency of an anti-symmetric mode.

2.2 Free vibration of a suspended cable attached to a transverse linear viscous damper

When analyzing a cable-damper system shown in Fig. 2-5, the key aspects the designers look for are the relationships between damper size, damping ratio and location and the amount of damping provided by the damper.

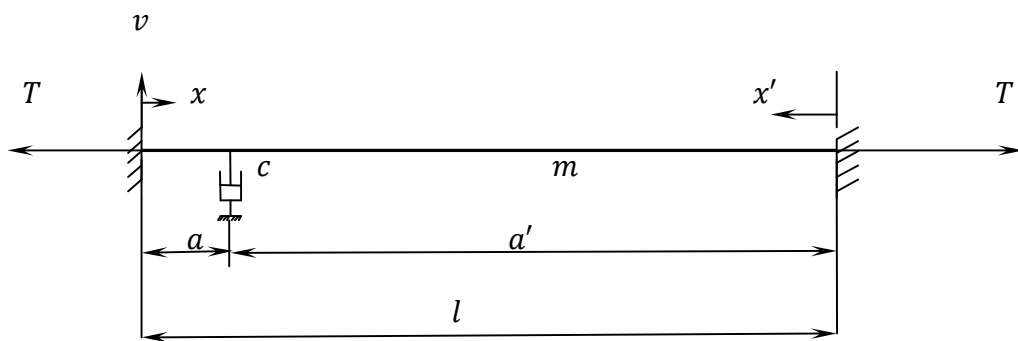


Figure 2-5 A taut cable with external linear viscous damper

Kovacs (1982) first identified the existence of optimum damping in a cable-damper system using a semi-empirical approach. According to the results, the maximum modal damping ratio attainable by a concentrated viscous damper was about half the relative distance of the damper from the cable support. i.e. $a/2l$ in Fig.2-5.

In a numerical analysis conducted by Yoneda & Maeda (1989) the existence of optimum damping was confirmed. Moreover an empirical formula was proposed by which the amount of damping in a cable-damper system could be estimated without resolving a complex eigenvalue problem. In this formulation the logarithmic decrement of the cable-damper system was related to the damping coefficient of the damper itself and the optimum achievable damping of the system.

By introducing a non dimensional damping coefficient, the empirical formula for predicting maximum attainable modal damping ratio based on damper location has been derived by Uno et al (1991).

Subsequently, a universal damping estimation curve was proposed by Pacheco et al (1993). It related the modal damping ratio of a cable-damper system, the mode number, the damper size, the damper location, unit mass, and fundamental frequency of the cable. They also confirmed the findings of Kovacs (1982) by investigating the frequency response curves when the damper coefficient equaled to zero, optimum and infinity.

The problem of controlling a vibrating horizontal string by a concentrated viscous damper was formulated by Krenk (2000) based on the assumption that the cable tension remained as a constant during oscillation. The equation of motion of the cable damper system shown in Fig. 2-5 is given by

$$T \frac{\partial^2 v}{\partial x^2} - m \frac{\partial^2 v}{\partial t^2} = c \frac{\partial v}{\partial t} \delta(x - a) \quad (2-16)$$

where T is the cable static tension, m is the mass density and c is the coefficient of the damper, respectively. The boundary conditions are $v(0, t) = 0$ and $v(l, t) = 0$. The discontinuity of slope at the location of damper results in the following equilibrium condition:

$$T \left(\left. \frac{\partial v}{\partial x} \right|_{a^+} - \left. \frac{\partial v}{\partial x} \right|_{a^-} \right) = c \frac{\partial v}{\partial t} \quad (2-17)$$

That is, the damper force at the damper location is treated as equal to the transverse force induced by cable tension due to discontinuity of slope at the location of damper. The coupling between the displacement space and time derivatives at damper location leads to complex mode shapes and frequencies of free vibration. It reveals that the eigen frequencies of the damped modes are complex, with the imaginary part representing the attenuation due to damping. By substituting the displacement function $v(x,t) = \bar{v}(x)e^{i\omega t}$ satisfying the boundary conditions and the continuity condition at damper location in Eq.(2-17), the following transcendental equation could be obtained for determination of eigen frequencies .

$$\cot(\beta a) + \cot(\beta a') = -i \frac{c}{\sqrt{Tm}} \quad (2-18)$$

$$\text{where } \omega = \sqrt{\frac{m}{T}}$$

The frequency ω could be obtained from Eq. (2-18) by simplifying the trigonometric functions using Taylor's expansion with the base value as the circular frequency of the cable. The solution will be a complex eigen frequency in the following form Krenk (2000)

$$\omega = \omega_n^0 [\sqrt{1 - \zeta^2} + i\zeta] \quad (2-19)$$

where ω_n^0 is the circular frequency of the cable in the n^{th} mode and ζ is the damping ratio.

A non-dimensional formulation was developed to calculate the vibration frequencies and the damping ratio for a stay cable equipped with a mechanical viscous damper by Tabatabai & Mehrabi (2000). The Bending stiffness and the sag extensibility of the cable were taken into account in the analysis. Non-dimensional parameters were defined based on a cable damper system as shown in Fig. 2-6 as follows.

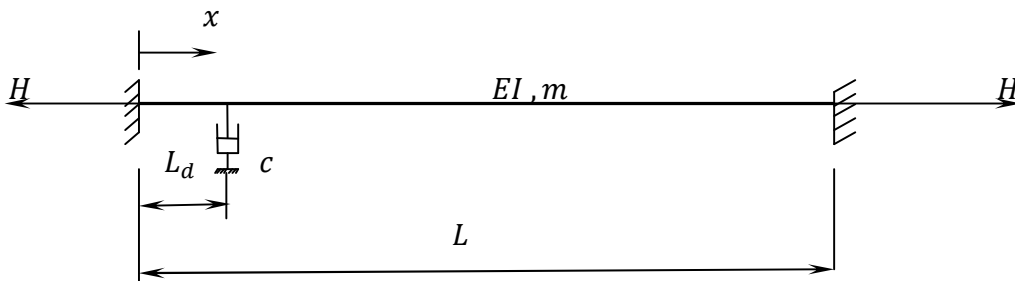


Figure 2-6 Layout of a cable-damper system

$$\xi = L\sqrt{H/EI} \quad (2-20)$$

$$\psi = \pi c/mL\omega_1 \quad (2-21)$$

$$\Gamma_d = L_d/L \quad (2-22)$$

where ξ is the bending stiffness parameter, ψ is the damping parameter, and Γ_d is the damper location parameter. The cable properties are as follows: H is the pretension, L is the length, m is the mass density, and EI is the bending stiffness. The damper properties are the damping coefficient c , and the damper location L_d . Practical ranges of these

parameters were established based on a data base of over 1400 bridge stay cables in 16 cable-stayed bridges in USA (Tabatabai & Mehrabi, 2000). It was observed that for more than 95% of cables in the field, the sag extensibility ratio is less than 1 and the effect of sag extensibility parameter λ^2 on performance of mechanical dampers was not very significant. Therefore sag extensibility could be treated as independent of the performance of mechanical damper. On the other hand, sag extensibility is the only parameter that represents the inclination of the cable in their formulation and hence they proposed that the performance of the mechanical damper is independent of the inclination of the cable.

Xu & Yu (1999) studied the non-linear behaviour of an inclined sag cable with respect to change in cable sag parameter and the effect of an oil damper on the cable vibration control using physical experiments. Results showed that an oil damper with an appropriately selected damping coefficient could effectively suppress non-linear in-plane cable motion.

An energy based approach to estimate the equivalent damping existed in a cable-damper system has been proposed (Cheng et al, 2010; Cheng & Koralalage, 2009 and Koralalage & Cheng, 2009). By introducing the kinetic energy decay ratio as a key index, the relation between the additional damping provided by an external damper and the kinetic energy dissipation rate of a damped cable was derived. The relationship of damper location, damper size, cable length, cable tension, cable bending stiffness, and equivalent cable model damping ratio was established. A set of damping estimation curves were developed as a design tool to assist external damper design for controlling bridge stay cable vibration.

In all the literature reviewed above, the support conditions at both cable ends are fixed. The movement of the bridge deck on real bridges and its impact on the behaviour of the cable and the damper are not taken into account. However, when the bridge span becomes longer and the bridge girder becomes more flexible, the motion at the cable-deck and damper-deck anchorage points can no longer be neglected. Its impact on the efficiency of the damper in controlling cable vibration can be considerable.

2.3 Free vibration of multi-span continuous uniform beams

The free vibration analysis of multi-span beams by considering different classical and non classical support conditions and various span combinations was conducted by Gorman (1975). The conventional beam differential equation was used in the analysis which expressed the equilibrium between the inertia forces and elastic restoring forces subjected to prescribed boundary conditions as given below. Figure 2-7 shows an element of a uniform beam under dynamic equilibrium.

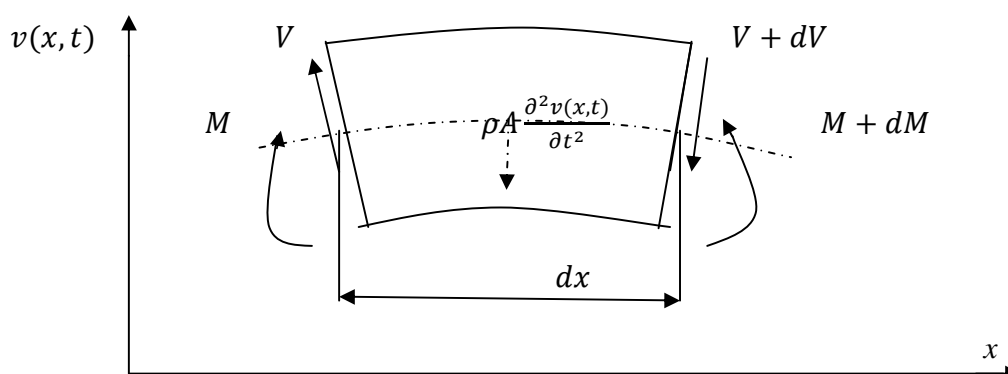


Figure 2-7 An element of a uniform beam subjected to vibration

The transverse shear force in the beam is given by

$$V = EI \frac{\partial^3 v(x,t)}{\partial x^3} \quad (2-23)$$

where EI is the bending stiffness of the beam and $v(x, t)$ is the transverse displacement of the beam. Considering the dynamic equilibrium of the beam element shown in Fig. 2-7, the net transverse shear force should be equal to the inertia force acting on the element.

Hence

$$-\frac{\partial^2 v(x,t)}{\partial t^2} = \frac{EI}{\rho A} \frac{\partial^4 (v(x,t))}{\partial x^4}. \quad (2-24)$$

The effect of shear strain and rotary inertia are neglected in the analysis. The Free vibration of a beam with intermediate point supports was studied by Kong & Cheung (1996) using Ritz method. The transverse displacement of the beam was approximated by a function comprised of a polynomial and a term of the conventional single span beam vibration function. Stiffness and mass matrices were formulated using the admissible trial functions, and the resulting linear eigen-equation was solved.

2.4 Effect of cable-deck interaction on vibration of a damped stay cable

Several researchers have studied theoretically and experimentally the internal resonance between the bridge global modes and the cable local modes which leads to highly unstable oscillation of stay cables. It has been observed that the angle of inclination of the stay cable plays a significant role in parametric excitation (Caetano,

2006). When the inclination angle is 0° , the cable is horizontal and the vibration excited by the deck vertical motion becomes a forced vibration whereas when the angle of inclination is 90° , the cable is vertical and deck motion creates a purely parametric effect without any forced vibration effect. When the cable inclination is between $0^{\circ} - 90^{\circ}$ the forced and parametric vibrations are coupled. The cable instability occurs when the vibration frequency of bridge deck is in the neighbourhood of twice the first natural frequency of the cable. In this case parametric vibration and forced vibration of stay cables are generally coupled. Such a parametric oscillation can be controlled by a damping system installed on the cable (Sun et al, 2003) . Based on the experiments conducted on the Second Severn Crossing in UK and the associated numerical analysis, Macdonald (2004) revealed that wind loads on cables can significantly affect global bridge response and since many combined cable-deck modes existed, cable and deck vibrations should not be considered separately.

The effects of girder vibration on the functionality of an external damper was investigated by Liang et al (2008). The cable was treated as a taut string and the bridge girder was simplified as a cantilever beam with the pylon end fixed as shown in Fig. 2-8 below. Results suggested that the girder vibration reduced the effectiveness of the damper as the cable length increases. In Fig. 2-8, AC represents the equivalent bridge girder, CD is the cable under investigation and BE represents the linear viscous damper. $u(x, t)$ is the horizontal component of the cable motion, $v(x, t)$ is the vertical component of cable motion and $w(x, t)$ is the vertical motion of the bridge girder.

This model, though considered cable-deck interaction in the formulation, the simplification of the bridge girder as a cantilever beam would lead to distorted dynamic

behaviour compared to the original bridge. In particular, the mode shapes of vibration are not represented correctly. This misrepresentation would directly affect the motions at cable-deck and damper-deck anchorage points and their relative relations. Therefore the

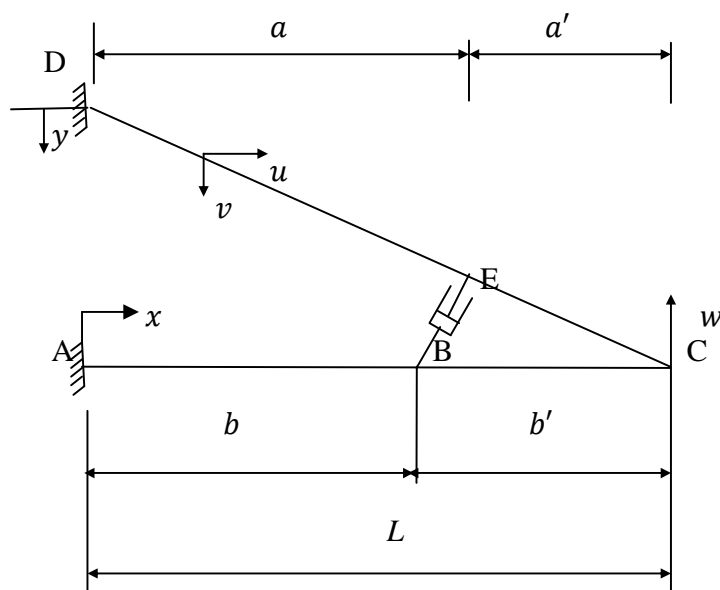


Figure 2-8 Simplified theoretical model of cable-deck-damper system (Liang et al, 2008)

impact of cable-deck interaction on the efficiency of the damper in controlling cable vibration cannot be reasonably simulated.

To the author's knowledge, the consideration of cable-deck interaction in evaluating dynamic behaviour of a damped cable has rarely been seen in the literature. To address this important issue, in particular, when designing dampers for cables in medium- to long-span cable-stayed bridges, a more accurate and reasonable analytical model of a cable-damper-deck system will be proposed. The details of the model and formulation will be presented in Chapter III.

CHAPTER III ANALYTICAL FORMULATION OF A CABLE- DAMPER-DECK COUPLED SYSTEM

In order to investigate the impact of cable-deck interaction on the damper efficiency to control cable vibration on cable-stayed bridge, an analytical model is developed in the current chapter. In the model, the bridge super-structure is modeled as a three-span continuous equivalent beam which has the same static and dynamic behaviour as the original bridge. A typical cable in the mid-span is included in the model. The cable is idealized as a taut cable, i.e. its bending stiffness is neglected in the analysis. An external damper is attached to the cable close to its anchorage point on the bridge deck. And it is considered as a linear viscous damper in the analysis.

In the following sections, the equations of motion and dynamic analyses of a single cable and a three-span continuous beam will be developed separately first. Then, the analytical formulation of the cable-damper-deck coupled system will be derived. A procedure to solve the equation of motion of the coupled system will also be proposed.

3.1 Free in-plane vibration of an inclined taut cable

3.1.1 Static Analysis

Figure 3-1(a) portrays an inclined suspended cable, the angle of inclination is θ . Fig.3-1(b) shows the static forces acting on an element of the cable of length ds .

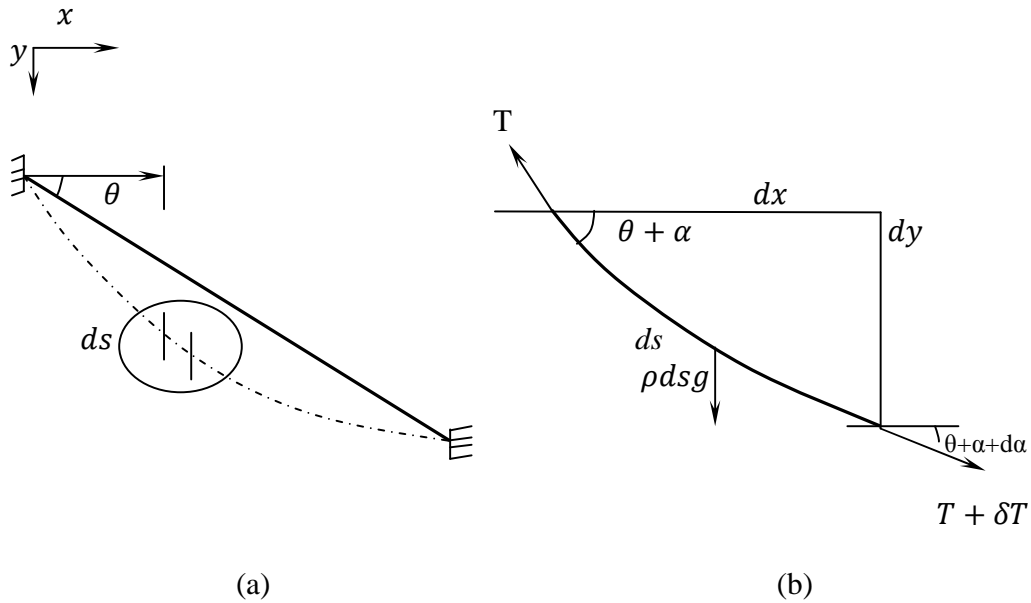


Figure 3-1 Static forces acting on an element of an inclined cable

Considering the static equilibrium of a cable element of length ds as shown in Fig. 3-1(b), the following relationships could be obtained:

$$\sum X = 0; (T + \delta T)\cos(\theta + \alpha + d\alpha) - T\cos(\theta + \alpha) = 0 \quad (3-1)$$

$$\sum Y = 0; (T + \delta T)\sin(\theta + \alpha + d\alpha) - T\sin(\theta + \alpha) + \rho ds g = 0 \quad (3-2)$$

where ρ is the mass density of the cable, g is the gravitational acceleration, T is the static tension of the cable, θ is the inclination angle of the cable with respect to the horizontal direction and $(\theta + \alpha)$ is the inclination of the cable element considered.

The geometric relationships for a small cable element of length ds are

$$\left\{ \begin{array}{l} \sin(\theta + \alpha) = \frac{dy}{ds} \\ \cos(\theta + \alpha) = \frac{dx}{ds} \\ ds = \sqrt{dx^2 + dy^2} \\ \frac{dx}{ds} = \frac{1}{\sqrt{1 + \frac{dy^2}{dx^2}}} \end{array} \right. \quad (3-3)$$

Substituting Eq.(3-3) into Eqs. (3-1) and (3-2), yields

$$\frac{d}{ds} \left[T \frac{dx}{ds} \right] = 0 \quad (3-4)$$

$$\frac{d}{ds} \left[T \frac{dy}{ds} \right] = -\rho g. \quad (3-5)$$

Equation (3-4) shows that the horizontal component of the cable tension, H , is a constant along the cable length, i.e.

$$H = T \frac{dx}{ds} = \text{constant} \quad (3-6)$$

3.1.2 Dynamic Analysis

The static equilibrium equations of a 2D inclined cable, Eqs. (3-4) and (3-5), can be further developed to dynamic equilibrium equations for in-plane motion of an inclined cable by the addition of dynamic terms to its horizontal displacement, x , vertical displacement, y , and tension, T , and incorporating the inertia force. The terms in the dynamic analysis are shown below.

	Static analysis	Dynamic analysis
Horizontal displacement	x	$x + u(x, t)$
Vertical displacement	y	$y + v(x, t)$
Cable tension	T	$T + \tau(x, t)$
Inertia force	No	$\rho \frac{\partial^2 u}{\partial t^2}, \rho \frac{\partial^2 v}{\partial t^2}$

where $u(x, t), v(x, t)$, and $\tau(x, t)$ are the additional horizontal displacement, additional vertical displacement and the additional cable tension induced by cable vibration respectively.

Replacing the static terms in Eq. (3-5) with the corresponding dynamic terms, the equation of motion for in-plane cable vibration in the vertical direction can be obtained as

$$\frac{d}{ds} \left\{ (T + \tau) \frac{d}{ds} [y(x) + v(x, t)] \right\} = -g + \rho \frac{\partial^2 v(x, t)}{\partial t^2} \quad (3-7)$$

Similarly, the equation of motion in the horizontal direction can be obtained as

$$\frac{d}{ds} \left\{ (T + \tau) \frac{d}{ds} [x + u(x, t)] \right\} = \rho \frac{\partial^2 u(x, t)}{\partial t^2} \quad (3-8)$$

Equation (3-7) can be simplified as follows with the assumption that the dynamic tension τ is negligible.

$$\frac{d}{ds} \left[T \frac{dy}{ds} \right] + \frac{d}{ds} \left[T \frac{dv(x,t)}{ds} \right] = -\rho g + \rho \frac{\partial^2 v(x,t)}{\partial t^2}$$

By eliminating static terms using (3-5) and writing the partial derivative term $\frac{d}{ds}$ with respect to dx ;

$$\frac{d}{dx} \left[T \frac{dv}{dx} \frac{dx}{ds} \right] \frac{dx}{ds} = \rho \frac{\partial^2 v}{\partial t^2}$$

Substituting Eqs. (3-3) and (3-6) into the above equation, leads to the relationship defining the in-plane vertical motion of an inclined taut string as

$$\frac{H}{\sqrt{1+\frac{dy^2}{dx^2}}} \frac{\partial^2 v}{\partial x^2} = \rho \frac{\partial^2 v}{\partial t^2} \quad (3-9)$$

Similarly the equation of motion of in-plane cable vibration in the horizontal direction is

$$\frac{d}{ds} \left\{ (T + \tau) \frac{d}{ds} [x + u(x, t)] \right\} = \rho \frac{\partial^2 u(x,t)}{\partial t^2} \quad (3-10)$$

Assume the dynamic tension τ is very small, gives

$$\frac{d}{ds} \left\{ T \left[\frac{dx}{ds} + \frac{du}{dx} \frac{dx}{ds} \right] \right\} = \rho \frac{\partial^2 u}{\partial t^2} \quad (3-11)$$

The equation of motion for horizontal in-plane vibration of an inclined taut cable can finally be expressed as follows by substituting Eqs.(3-3) and (3-6) into Eq.(3-11);

$$\frac{H}{\sqrt{1+\frac{dy^2}{dx^2}}} \frac{\partial}{\partial x} \left(1 + \frac{du}{dx} \right) = \rho \frac{\partial^2 u}{\partial t^2} \quad \rightarrow \quad \frac{H}{\sqrt{1+\frac{dy^2}{dx^2}}} \frac{\partial^2 u}{\partial x^2} = \rho \frac{\partial^2 u}{\partial t^2} \quad (3-12)$$

3.1.3 Numerical example

The equations of motion derived in Section 3.1.2 are verified by a numerical example and compared with that of Irvine (1980).

In an experimental cable setup, a horizontal cable of length $L = 13.695$ m and unit mass of cable $\rho = 3.6$ kg/m was used under static cable tension of $H = 122.1$ kN. It is intended to determine the first modal frequency of the cable for in-plane vertical motion. The cable is idealized as a taut string.

3.1.3.1 Application of Eq. (3.9)

Since the cable is suspended horizontally and there is negligible sag, $\frac{dy}{dx} = 0$. Hence Eq. (3.9) becomes

$$H \frac{\partial^2 v}{\partial x^2} = \rho \frac{\partial^2 v}{\partial t^2} \quad (3-13)$$

Substituting $v(x, t) = \bar{v}(x)q(t)$ to separate variables in Eq. (3-13) we obtain

$$H \frac{\bar{v}''(x)}{\bar{v}(x)} = \rho \frac{\ddot{q}(t)}{q(t)} = k \quad (3-14)$$

where k is a constant.

Equation (3-14) can be written as two separate equations as follows

$$H\bar{v}''(x) - k\bar{v}(x) = 0 \quad (3-15)$$

$$\rho\ddot{q}(t) - kq(t) = 0 \quad (3-16)$$

The solution for Eq. (3-15) is in the form of

$$\bar{v}(x) = A \sin \beta x + B \cos \beta x \quad (3-17)$$

where A, B and β are constants.

Since the cable is suspended horizontally and fixed at both ends, $w(0) = 0$ and $w(L) = 0$. Using these boundary conditions in Eq. (3-17) leads to $B = 0$ and $\sin \beta L = 0$ since $A \neq 0$
 $\rightarrow \beta L = n\pi$ or $\beta = \frac{n\pi}{L}$ where $n = 1, 2, 3, \dots$

Substituting $\bar{v}(x) = A \sin \beta x$ in Eq. (3-15), the following result is obtained

$$[\beta^2 - \frac{k}{H}] \bar{v}(x) = 0 \quad (3-18)$$

Hence for non trivial solution of $\bar{v}(x)$, $k = \beta^2 H = \frac{n^2 \pi^2}{L^2} H$. Similarly, using

equation (3-16), it can be shown that if

$$q(t) = P \sin \omega t \quad (3-19)$$

$$[\omega^2 - \frac{k}{\rho}]q(t) = 0 \quad (3-20)$$

where P is a constant and ω is the circular frequency of cable vibration.

Using Eq. (3-20), for nontrivial solution of $u(t)$

$$\omega = \sqrt{\frac{k}{\rho}} = \frac{n\pi}{L} \sqrt{\frac{H}{\rho}} \quad (3-21)$$

The frequency of vibration is given by

$$f = \frac{\omega}{2\pi} = \frac{n}{2L} \sqrt{\frac{H}{\rho}}, n = 1, 2, 3, .. \quad (3-22)$$

Substituting $H = 122100N$, $\rho = 3.6 \text{ kg/m}$ and $L = 13.695 \text{ m}$ into Eq. (3-22), the first modal frequency ($n = 1$) is $f = 6.72 \text{ Hz}$.

3.1.3.2 Irvine's approach

The first mode is the symmetric first mode of vertical in-plane motion. Since the cable is a taut string, the Irvine parameter $\lambda^2 = 0$. The transcendental equation becomes $n \frac{\tilde{\omega}}{2} = -\infty$,

where $\tilde{\omega} = \omega L / (H/\rho)^{\frac{1}{2}}$. Hence $\tilde{\omega} = \pi \rightarrow \omega = \frac{\pi}{L} \sqrt{\frac{H}{\rho}} \rightarrow f = \frac{1}{2L} \sqrt{\frac{H}{\rho}}$ substitute into H, ρ, L yields $f = 6.72\text{Hz}$. Since both approaches gave the same results, the derivations in Section 3.1.2 are correct.

3.2 Free vibration analysis of a three-span continuous beam

3.2.1 Equation of motion for in-plane vibration

A three-span continuous beam with simply supported ends is considered for the analysis. The mass density and the bending stiffness of the beam are assumed to be uniform through all the spans. The effects of shear strain and rotary inertia are neglected in the analysis. Schematic diagram of the beam considered in the analysis is shown in Figure 3-2.

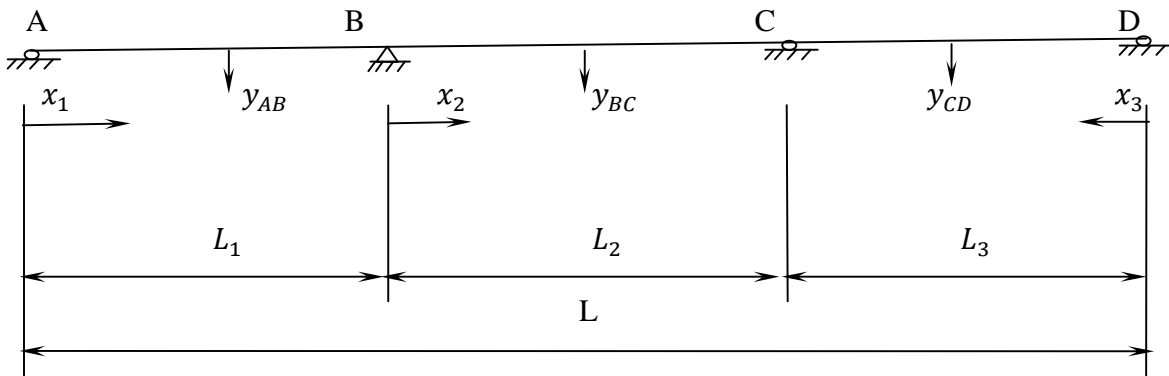


Figure 3-2 schematic diagram of a three-span continuous beam

The motion of the beam can be described by Eq. (2-34)

$$-\frac{\partial^2 y(x,t)}{\partial t^2} = \frac{EI}{m} \frac{\partial^4 y(x,t)}{\partial x^4} \quad (3-23)$$

where m is the mass density of the beam, EI is the beam bending stiffness and $y(x, t)$ is the vertical in-plane displacement of the beam with respect to its static profile.

Substituting $y(x, t) = v(x)q(t)$ and substitute it into Eq. (3-23), and rearranging the terms, we obtain

$$EI \frac{v^{iv}(x)}{v(x)} = -m \frac{\ddot{q}(t)}{q(t)} = k \quad (3-24)$$

where $v^{iv}(x)$ represents the fourth derivative of $v(x)$ with respect to x , $\ddot{q}(t)$ is the second derivative of $q(t)$ with respect to t and k is a constant.

Equation (3-24) can be re-written as two separate equations as follows:

$$EI v^{iv}(x) - kv(x) = 0 \quad (3-25)$$

$$\ddot{q}(t) + \frac{k}{m} q(t) = 0 \quad (3-26)$$

The solution to Eq.(3-25) for the i^{th} span ($i = 1,2,3$) will be given by the shape function

$$v_i(x_i) = A_i \sin \lambda x_i + B_i \cos \lambda x_i + C_i \sinh \lambda x_i + D_i \cosh \lambda x_i, i = 1,2,3 \quad (3-27)$$

where A_i, B_i, C_i, D_i are coefficients of shape function $v_i(x_i)$ of the i^{th} span ($i = 1,2,3$), and λ is the eigenvalue.

Using non-dimensional form $\xi_i = \frac{x_i}{L}$ and substituting Eq. (3-27) to Eq.(3-25) gives

$$[\lambda^4 - \frac{kL^4}{EI}]v_i(\xi_i) = 0 \quad (3-28)$$

For nontrivial solutions of $v_i(\xi_i)$, Eq. (3-28) should satisfy ;

$$k = \lambda^4 EI / L^4 \quad (3-29)$$

where L is the total length of the beam.

The solution to Eq. (3-26) is assumed to have the form of

$$q(t) = P \sin \omega t \quad (3-30)$$

where P is constant and ω represents the frequency of vibration of the beam. Substituting the value of $v(t)$ from Eq. (3-20) in Eq. (3-16) yields

$$\omega = \sqrt{\frac{k}{m}} \quad (3-31)$$

Substituting Eq. (3-29) into Eq. (3-31) gives

$$\omega = \frac{\lambda^2}{L^2} \sqrt{\frac{EI}{m}} \quad (3-32)$$

Boundary conditions and compatibility conditions: (please refer to Fig. 3-2)

1. Boundary conditions:

$$\text{Displacement at A: } [v_{AB}]_{x_1=0} = 0; \rightarrow B_1 + D_1 = 0 \quad (3-33)$$

$$\text{Moment at A: } [v''_{AB}]_{x_1=0} = 0; \rightarrow -B_1 + D_1 = 0 \quad (3-34)$$

Combining the above two equations, yields

$$B_1 = D_1 = 0 \quad (3-35)$$

Displacement at B:

$$[v_{AB}]_{x_1=L_1} = 0; A_1 \sin \lambda L_1 + C_1 \sinh \lambda L_1 = 0; C_1 = -\frac{\sin \lambda L_1}{\sinh \lambda L_1} A_1 \quad (3-36)$$

Using results (3-35) and (3-36);

$$v_{AB} = A_1 \left[\sin \lambda x_1 - \frac{\sin \lambda L_1}{\sinh \lambda L_1} \sinh \lambda x_1 \right] \quad (3-37)$$

Due to the symmetry of the structure, v_{DC} for span CD can be similarly derived as

$$v_{DC} = A_3 \left[\sin \lambda x_3 - \frac{\sin \lambda L_3}{\sinh \lambda L_3} \sinh \lambda x_3 \right] \quad (3-38)$$

$$\text{Displacement at B : } [v_{BC}]_{x_2=0} = 0; \rightarrow B_2 + D_2 = 0 \rightarrow D_2 = -B_2 \quad (3-39)$$

Displacement at C ;

$$\rightarrow [v_{BC}]_{x_2=L_2} = 0; \rightarrow A_2 \sin \lambda L_2 + B_2 [\cos \lambda L_2 - \cosh \lambda L_2] + C_2 \sinh \lambda L_2 = 0 \quad (3-40)$$

2. Compatibility conditions:

Slope at B:

$$[v'_{BC}]_{x_2=0} = [v'_{AB}]_{x_1=L_1} \rightarrow A_1 \left[\cos \lambda L_1 - \frac{\sin \lambda L_1}{\sinh \lambda L_1} \cosh \lambda L_1 \right] - A_2 - C_2 = 0 \quad (3-41)$$

Slope at C: $[v'_{BC}]_{x_2=L_2} = -[v'_{DC}]_{x_3=L_3} \rightarrow$

$$A_2 \cos \lambda L_2 + A_3 \left[\cos \lambda L_3 - \frac{\sin \lambda L_3}{\sinh \lambda L_3} \cosh \lambda L_3 \right] - B_2 [\sin \lambda L_2 + \sinh \lambda L_2] + C_2 \cosh \lambda L_2 = 0 \quad (3-42)$$

$$\text{Moment at B: } [EIv''_{BC}]_{x_2=0} = [EIv''_{AB}]_{x_1=L_1} \rightarrow B_2 = A_1 \sin \lambda L_1 \quad (3-43)$$

$$\text{Moment at C: } [EIv''_{BC}]_{x_2=L_2} = [EIv''_{DC}]_{x_3=L_3}$$

$$\rightarrow -A_2 \sin \lambda L_2 + 2A_3 \sin \lambda L_3 - B_2 [\cos \lambda L_2 + \cosh \lambda L_2] + C_2 \sinh \lambda L_2 = 0 \quad (3-44)$$

$$\text{From Eqs. (3-40) and (3-43): } C_2 = -A_1 \sin \lambda L_1 \phi - A_2 \theta \quad (3-45)$$

where $\theta = \frac{\sin \lambda L_2}{\sinh \lambda L_2}$ and $\phi = (\cos \lambda L_2 - \cosh \lambda L_2) / \sinh \lambda L_2$

Substituting Eqs. (3-43) and (3-45) into (3-41),(3-42) and (3-44) leads to

$$\begin{bmatrix} \cos\lambda L_1 - \sin\lambda L_1 \coth\lambda L_1 + \phi \sin\lambda L_1 \\ \sin\lambda L_1 [\sin\lambda L_2 + \sinh\lambda L_2 + \phi \cosh\lambda L_2] \\ \sin\lambda L_1 \cos\lambda L_2 \end{bmatrix} \begin{vmatrix} \theta - 1 \\ \theta \cosh\lambda L_2 - \cos\lambda L_2 \\ \sin\lambda L_2 \end{vmatrix} \begin{bmatrix} 0 \\ - \\ -\sin\lambda L_3 \end{bmatrix} \begin{bmatrix} \cos\lambda L_3 + \sin\lambda L_3 \coth\lambda L_3 \\ \\ \end{bmatrix} \begin{bmatrix} A_1 \\ A_2 \\ A_3 \end{bmatrix} = \begin{bmatrix} 0 \\ 0 \\ 0 \end{bmatrix} \quad (3-46)$$

It is in the form $[G]\{S\}=\{0\}$, where $\{S\}=[A_1 \ A_2 \ A_3]'$, $\{0\}$ is the null matrix and

$$[G] = \begin{bmatrix} \cos\lambda L_1 - \sin\lambda L_1 \coth\lambda L_1 + \phi \sin\lambda L_1 \\ \sin\lambda L_1 [\sin\lambda L_2 + \sinh\lambda L_2 + \phi \cosh\lambda L_2] \\ \sin\lambda L_1 \cos\lambda L_2 \end{bmatrix} \begin{vmatrix} \theta - 1 \\ \theta \cosh\lambda L_2 - \cos\lambda L_2 \\ \sin\lambda L_2 \end{vmatrix} \begin{bmatrix} 0 \\ - \\ -\sin\lambda L_3 \end{bmatrix} \begin{bmatrix} \cos\lambda L_3 + \sin\lambda L_3 \coth\lambda L_3 \\ \\ \end{bmatrix}$$

For nontrivial solutions of $A_i (i = 1,2,3)$, the $\det|G|$ should be zero. This condition will yield the results of eigenvalues λ_i and eigenvectors. The natural frequency of the beam can thus be determined from $f_i = \frac{\lambda_i^2}{L^2} \sqrt{EI/m}$ and the mode shape is the corresponding eigenvectors.

3.2.2 Numerical Example

Consider a three-span continuous bridge with span lengths 50m, 100m and 60m as shown in Fig. 3-3. The ends of the bridge are simply supported and the two middle supports are continuous. The average mass per unit length of the bridge along its longitudinal axis is $m = 3000 \text{ kg}$. The bending stiffness of the bridge is $EI = 1.5 \times 10^{11} \text{ Nm}^2$. It is intended to find the natural frequency of the bridge.

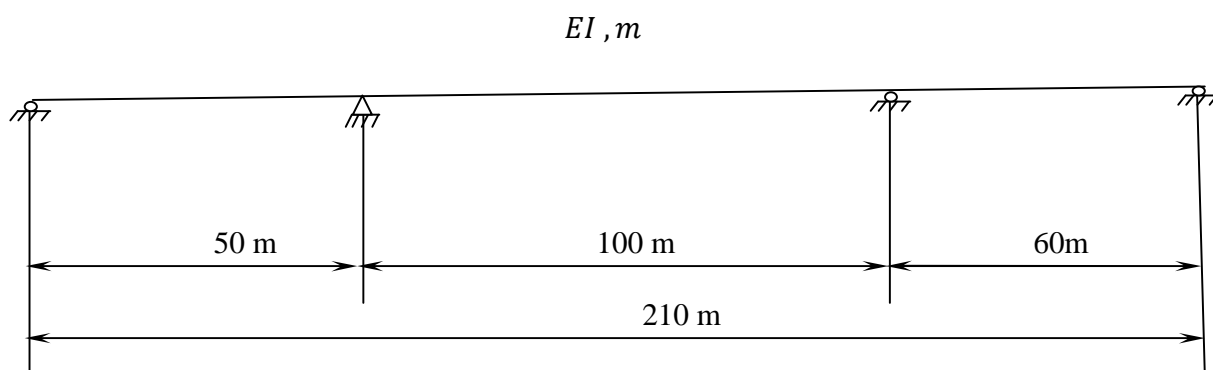


Figure 3-3 Schematic diagram of a three-span continuous beam

Solution: Substituting $L_1 = 50, L_2 = 100, L_3 = 60$ in the developed Matlab program to resolve Eq. (3-46) gives the following graphical solution for λ_1

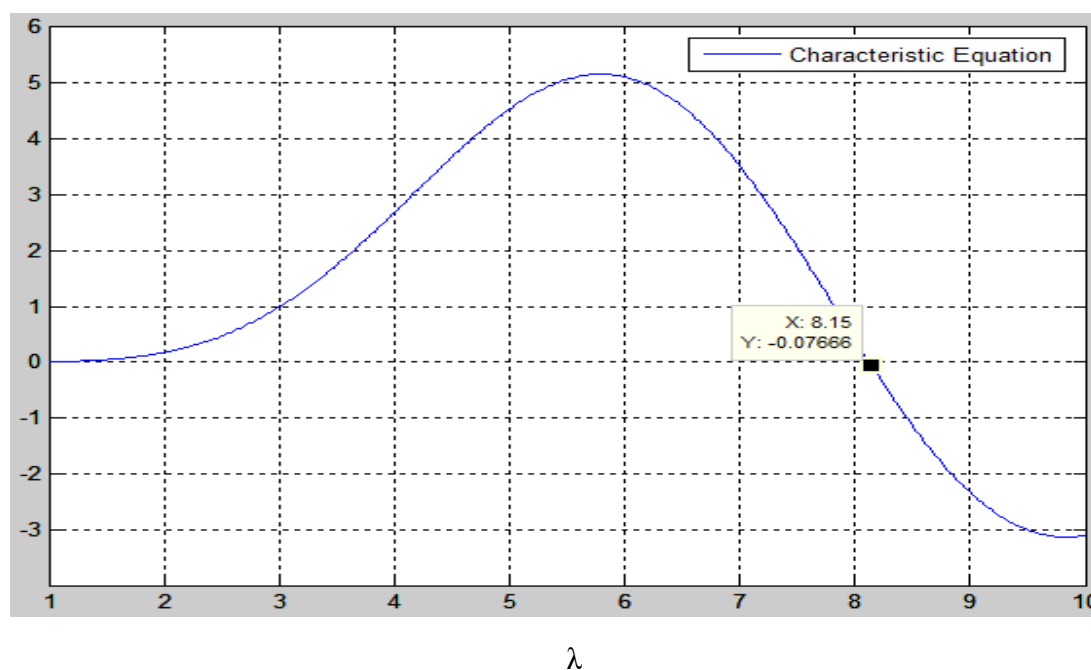


Figure 3-4 Graph of $\text{Det}[G]$ vs λ

Figure 3-4 shows eigenvalue $\lambda_1 = 8.15$. Substitute, $\lambda_1 = 8.15, L = 210 \text{ m}, EI = 1.5 \times 10^{11} \text{ Nm}^2, m = 3000 \text{ kg}$ into Eq. (3-32) gives $\omega = 10.65 \text{ rad/s}$ and the natural frequency of in-plane vertical vibration of the bridge is $f = 1.69 \text{ Hz}$.

Gorman (1975) carried out free vibration analysis of beams with multiple spans and different support conditions. The results of this example is compared with that obtained from the tabulated eigenvalues by Gorman (1975) as follows:

Using non-dimensional parameters $\xi_1 = 0.24$, $\xi_2 = 0.48$, $\xi_3 = 0.28$ in triple-span simply-supported beam table to get $\lambda_1 = 8.082$. Substituting λ_1, L, m and EI into Eq. (3-32) gives $\omega = 10.47\text{rad/s}$ and $f = 1.67\text{ Hz}$

The results from the derived model agrees well with that of Gorman (1975).

3.3 Equation of motion of cable-damper-deck coupled system

To consider cable-deck interaction in analyzing the controlling effect of an external damper on cable vibration, the single cable in section 3.1 and the three-span continuous beam in section 3.2 and a linear viscous damper are integrated in this section to derive equation of motion of a cable-damper-deck coupled system. The system is shown schematically in Fig.3-5.

The mathematical model in this analysis comprised of an isolated bridge stay cable HD, an equivalent three-span continuous beam ABCDEF which represents the bridge superstructure along with all the other cable supports except cable HD, and a linear viscous damper attached to the cable at G. Cable HD has a fixed support at H, the pylon end and a vertically moving support at D, the bridge girder end. The equivalent beam ABCDEF is simply supported at ends A and F, and two intermediate supports are at B and E. The linear viscous damper is attached to the cable at G and supported on bridge girder at C as shown in Figure 3-5.

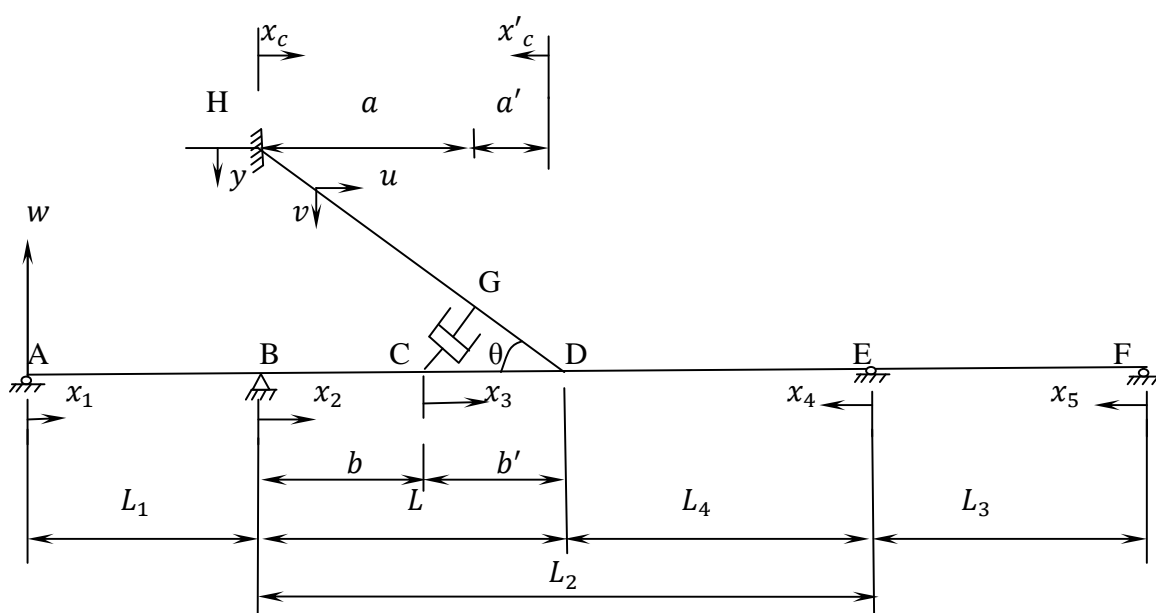


Figure3-5 schematic diagram of the theoretical model of cable-deck- damper system

The following basic assumptions are made in order to simplify the analysis.

- The axial deformation of the bridge girder can be neglected. Only vertical movements due to bridge girder vibration are considered.
- The bridge girder is idealized as a three-span continuous equivalent beam which has uniform mass density and flexural rigidity over the entire span.
- For the three-span equivalent continuous beam, the static deflection at the cable-deck anchorage and the fundamental frequency are assumed to be the same as the original bridge superstructure.
- The static deflection at point D, where the cable is anchored to the bridge girder, is assumed to be zero.
- The cable is assumed as a tensioned taut string. The effect of sag and bending stiffness are not considered in the formulation.

- Only in-plane vibrations of cable, deck are considered. Shear and torsional effects of bridge girder are neglected.
- The damper is a linear viscous damper.

By neglecting the dynamic tension, the equation of motion for free vibration of undamped taut inclined cable, is given similar to (3.9) and (3.12) by

$$\text{Horizontal : } \frac{H}{\sqrt{1+\left(\frac{dy}{dx}\right)^2}} \frac{\partial^2 u}{\partial x^2} = m_1 \frac{\partial^2 u}{\partial t^2} \quad (3-47)$$

$$\text{Vertical: } \frac{H}{\sqrt{1+\left(\frac{dy}{dx}\right)^2}} \frac{\partial^2 v}{\partial x^2} = m_1 \frac{\partial^2 v}{\partial t^2} \quad (3-48)$$

where H is the horizontal component of cable tension T , m_1 is the mass density of the cable, u, v are the horizontal and vertical displacements of cable from its static configuration, respectively.

Considering the damping force acting on the cable, and substituting $\frac{dy}{dx} = \tan\theta$ in Eq. (3-47) above;

$$T \cos^2 \theta \frac{\partial^2 u(x,t)}{\partial x^2} - m_1 \frac{\partial^2 u(x,t)}{\partial t^2} = -F_u \delta(x_c - a) \quad (3-49)$$

Similarly considering vertical motion of the cable and the damping force in the vertical direction, Eq. (3-48) can be written as

$$T \cos^2 \theta \frac{\partial^2 v(x,t)}{\partial x^2} - m_1 \frac{\partial^2 v(x,t)}{\partial t^2} = -F_v \delta(x_c - a) \quad (3-50)$$

Considering the vertical motion of the bridge girder and the damping force acting on it, the equation of motion of the bridge girder with the existence of an external damper can be given by

$$EI \frac{\partial^4 w(x,t)}{\partial x^4} + m_2 \frac{\partial^2 w(x,t)}{\partial t^2} = -F_w \delta(x_2 - b) \quad (3-51)$$

where δ is the dirac delta function, EI is the bending stiffness of the bridge girder, m_2 is the mass density of the bridge girder, F_u is the force exerted by the damper on the cable in the horizontal direction at point G, F_v is the force exerted by the damper on the cable in vertical direction at point G and F_w is the force exerted by the damper on the bridge girder in the vertical direction at point C respectively.

Since the damping force exerted on the cable is equivalent to the transverse force induced by cable tension due to discontinuity of slope at the damper location, the following expressions can be used to express the damping force on the cable in the horizontal and vertical directions.

$$T \sin \theta \left\{ \left[\frac{\partial u(x,t)}{\partial x} \right]_{a^+} - \left[\frac{\partial u(x,t)}{\partial x} \right]_{a^-} \right\} = -F_u \quad (3-52)$$

$$T \cos \theta \left\{ \left[\frac{\partial v(x,t)}{\partial x} \right]_{a^+} - \left[\frac{\partial v(x,t)}{\partial x} \right]_{a^-} \right\} = -F_v \quad (3-53)$$

The change in shear force on the location of the damper is the damping force acting on the girder. Hence

$$EI \left\{ \left[\frac{\partial w^3(x,t)}{\partial x^3} \right]_{b^-} - \left[\frac{\partial w^3(x,t)}{\partial x^3} \right]_{b^+} \right\} = -F_w \quad (3-54)$$

Based on the assumption of a linear viscous damper, the damping force developed in the damper in the horizontal and vertical directions are

$$-C \frac{du(a,t)}{dt} = F_u \quad (3-55)$$

$$-C \left[\frac{dv(a,t)}{dt} - \frac{dw(b,t)}{dt} \right] = F_v = -F_w \quad (3-56)$$

where C is the damping coefficient in N-s/m.

The following form of solutions are assumed for u , v and w

$$u(x,t) = \bar{u}(x)e^{i\omega t} \quad (3-57)$$

$$v(x,t) = \bar{v}(x)e^{i\omega t} \quad (3-58)$$

$$w(x,t) = \bar{w}(x)e^{i\omega t} \quad (3-59)$$

where the shape function $\bar{w}(x)$ is defined as $\bar{w}_{AB}(x_1)$ for $0 \leq x_1 \leq L_1$; $\bar{w}_{BC}(x_2)$ for $0 \leq x_2 \leq b$; $\bar{w}_{CD}(x_3)$ for $0 \leq x_3 \leq b'$; $\bar{w}_{ED}(x_4)$ for $0 \leq x_4 \leq L_4$; $\bar{w}_{FE}(x_5)$ for $0 \leq x_5 \leq L_3$. The shape

function $\bar{v}(x)$ is defined as $\bar{v}_{HG}(x_c)$ for $0 \leq x_c \leq a$; $\bar{v}_{DG}(x'_c)$ for $0 \leq x'_c \leq a_1$. And the shape function $\bar{u}(x)$ is defined as $\bar{u}_{HG}(x_c)$ for $0 \leq x_c \leq a$; $\bar{u}_{DG}(x'_c)$ for $0 \leq x'_c \leq a_1$

where $x_1, x_2, x_3, x_4, x_5, x_c$ and x'_c are the local coordinates measured from the direction indicated in Fig.3-5. They are introduced for the convenience of derivation.

Substituting Eqs. (3-57)-(3-59) into Eqs. (3-52)-(3-54) gives

$$\frac{d^2 \bar{u}(x)}{dx^2} + \frac{m_1 \omega^2}{T \cos^2 \theta} \bar{u}(x) = C \frac{[\bar{u}_{HG}(a)] i \omega \delta(x_c - a)}{T \cos^2 \theta} \quad (3-60)$$

$$\frac{d^2 \bar{v}(x)}{dx^2} + \frac{m_1 \omega^2}{T \cos^2 \theta} \bar{v}(x) = C \frac{[\bar{v}_{HG}(a) - \bar{w}_{BC}(b)] i \omega \delta(x_c - a)}{T \cos^2 \theta} \quad (3-61)$$

$$\frac{d^4 \bar{w}(x)}{dx^4} - \frac{m_2}{EI} \bar{w}(x) \omega^2 = C \frac{[\bar{w}_{BC}(b) - \bar{v}_{HG}(a)]}{EI} i \omega \delta(x_2 - b) \quad (3-62)$$

The boundary conditions, compatibility conditions and initial conditions of the cable-damper –deck system shown in Fig.(3-5) are;

i) Span AB

$$\text{Displacement at A: } \bar{w}_{AB}(0) = 0 \quad (3-63-a)$$

$$\text{Moment at A: } \bar{w}_{AB}''(0) = 0 \quad (3-63-b)$$

$$\text{Continuity of slope at B: } \bar{w}'_{AB}(L_1) = \bar{w}'_{BC}(0) \quad (3-63-c)$$

$$\text{Continuity of moment at B: } \bar{w}''_{AB}(L_1) = \bar{w}''_{BC}(0) \quad (3-63-d)$$

$$\text{Displacement at B: } \bar{w}_{AB}(L_1) = 0 \quad (3-63-e)$$

ii) Span BC

$$\text{Displacement at B: } \bar{w}_{BC}(0) = 0 \quad (3-63-f)$$

$$\text{Continuity of displacement at C: } \bar{w}_{BC}(b) = \bar{w}_{CD}(0) \quad (3-63-g)$$

$$\text{Continuity of slope at C: } \bar{w}'_{BC}(b) = \bar{w}'_{CD}(0) \quad (3-63-h)$$

$$\text{Continuity of moment at C: } \bar{w}''_{BC}(b) = \bar{w}''_{CD}(0) \quad (3-63-i)$$

iii) Span CD

$$\text{Shear at C: } w'''_{CD}(0, t) - w'''_{BC}(b, t) = -C[\dot{w}_{BC}(b) - \dot{v}(b)]/(EI) \quad (3-63-j)$$

$$\text{Continuity of displacement at D: } \bar{w}_{CD}(b') = \bar{w}_{ED}(L_4) \quad (3-63-k)$$

$$\text{Continuity of slope at D: } \bar{w}'_{CD}(b') = -\bar{w}'_{ED}(L_4) \quad (3-63-l)$$

$$\text{Continuity of moment at D: } \bar{w}''_{CD}(b') = \bar{w}''_{ED}(L_4) \quad (3-63-m)$$

Shear at D:

$$EIw'''_{CD}(b', t) + EIw'''_{ED}(L_4, t) = -T \cos \theta \frac{\partial v_{DG}(0, t)}{\partial x} \quad (3-63-n)$$

iv) Span DE

$$\text{Displacement at E: } \bar{w}_{ED}(0) = 0 \quad (3-63-p)$$

$$\text{Slope continuity at E: } \bar{w}'_{FE}(L_3) = \bar{w}'_{ED}(0) \quad (3-63-q)$$

$$\text{Moment continuity at E: } \bar{w}''_{FE}(L_3) = \bar{w}''_{ED}(0) \quad (3-63-r)$$

v) Span EF

$$\text{Displacement at E: } \bar{w}_{FE}(L_3) = 0 \quad (3-63-s)$$

$$\text{Displacement at F: } \bar{w}_{FE}(0) = 0 \quad (3-63-t)$$

$$\text{Moment at F: } \bar{w}''_{FE}(0) = 0 \quad (3-63-u)$$

vi) Cable

$$\text{Horizontal displacement at H: } \bar{u}_{HG}(0) = 0 \quad (3-64-a)$$

$$\text{Vertical displacement at H: } \bar{v}_{HG}(0) = 0 \quad (3-64-b)$$

$$\text{Horizontal displacement at G: } \bar{u}_G(a) = \bar{u}_{DG}(a') \quad (3-64-c)$$

$$\text{Vertical displacement at G: } \bar{v}_{HG}(a) = \bar{v}_{DG}(a') \quad (3-64-d)$$

$$\text{Continuity of vertical displacement at D: } \bar{v}_{DG}(0) = \bar{w}_{CD}(b') \quad (3-64-e)$$

$$\text{Horizontal displacement at D: } \bar{u}_{DG}(0) = 0 \quad (3-64-f)$$

Horizontal component of damping force on cable at G:

$$T \sin \theta \left\{ \left[\frac{\partial u(x,t)}{\partial x} \right]_{a^+} - \left[\frac{\partial u(x,t)}{\partial x} \right]_{a^-} \right\} = C \frac{du(a,t)}{dt} \quad (3-64-g)$$

Vertical damping force on cable at G:

$$T \cos \theta \left\{ \left[\frac{\partial v(x,t)}{\partial x} \right]_{a^+} - \left[\frac{\partial v(x,t)}{\partial x} \right]_{a^-} \right\} = C \left\{ \frac{dv(a,t)}{dt} - \frac{dw(b,t)}{dt} \right\} \quad (3-64-h)$$

The assumed forms of solution for the shape functions are

$$\bar{w}_{AB}(x_1) = A_1 \sin \lambda x_1 + B_1 \cos \lambda x_1 + C_1 \sinh \lambda x_1 + D_1 \cosh \lambda x_1 \quad (3-65-a)$$

$$\bar{w}_{BC}(x_2) = A_2 \sin \lambda x_2 + B_2 \cos \lambda x_2 + C_2 \sinh \lambda x_2 + D_2 \cosh \lambda x_2 \quad (3-65-b)$$

$$\bar{w}_{CD}(x_3) = A_3 \sin \lambda x_3 + B_3 \cos \lambda x_3 + C_3 \sinh \lambda x_3 + D_3 \cosh \lambda x_3 \quad (3-65-c)$$

$$\bar{w}_{ED}(x_4) = A_4 \sin \lambda x_4 + B_4 \cos \lambda x_4 + C_4 \sinh \lambda x_4 + D_4 \cosh \lambda x_4 \quad (3-65-d)$$

$$\bar{w}_{FE}(x_5) = A_5 \sin \lambda x_5 + B_5 \cos \lambda x_5 + C_5 \sinh \lambda x_5 + D_5 \cosh \lambda x_5 \quad (3-65-e)$$

$$\bar{v}_{HG}(x'_c) = P_1 \sin \gamma x_c + Q_1 \cos \gamma x_c \quad (3-65-f)$$

$$\bar{v}_{DG}(x'_c) = P_2 \sin \gamma x'_c + Q_2 \cos \gamma x'_c \quad (3-65-g)$$

where A_i, B_i, C_i, D_i , ($i = 1, 2, 3, 4, 5$), P_1, P_2, Q_1 and Q_2 are constants.

For $0 \leq x_c < a$, substituting $v(x, t) = \bar{v}_{HG} e^{i\omega t}$ into Eq. (3-61), gives

$$\bar{v}_{HG}''(x_c) + \frac{m_1 \omega^2}{T \cos^2 \theta} \bar{v}_{HG}(x_c) = 0 \quad (3-66)$$

Substituting Eq.(3-65-f) into Eq.(3-66) yields

$$\left[-\gamma^2 + \frac{m_1 \omega^2}{T \cos^2 \theta} \right] \bar{v}_{HG}(x_c) = 0$$

The eigenvalue γ can be thus found as

$$\gamma = \frac{\omega}{\cos \theta} \sqrt{\frac{m_1}{T}} \quad (3-67)$$

where ω is the frequency of vibration of the system.

Referring to Eq. (3-32)

$$\lambda = \sqrt[4]{\frac{\omega^2 m_2}{EI}} \quad (3-68)$$

The assumed solutions for the shape functions are substituted in the boundary conditions, Eqs.

(3-63-a) to (3-63-u) to determine the unknown coefficients,

$A_i, B_i, C_i, D_i, (i = 1,2,3,4,5), P_1, P_2, Q_1$ and Q_2 .

$$\bar{w}_{AB}(0) = 0: \quad B_1 + D_1 = 0 \quad (3-69)$$

$$\bar{w}_{AB}''(0) = 0: \quad -B_1 + D_1 = 0 \quad (3-70)$$

Combining Eqs. (3-69) and (3-70) it can be found that

$$B_1 = D_1 = 0 \quad (3-71)$$

$$\bar{w}_{AB}(L_1) = 0: \quad A_1 \sin \lambda L_1 + C_1 \sinh \lambda L_1 = 0; \rightarrow C_1 = -\frac{\sin \lambda L_1}{\sinh \lambda L_1} A_1 \quad (3-72)$$

$$\bar{w}'_{AB}(L_1) = w'_{BC}(0): \quad A_1 \left[\cos \lambda L_1 - \frac{\cosh \lambda L_1}{\sinh \lambda L_1} \sin \lambda L_1 \right] - A_2 - C_2 = 0 \quad (3-73)$$

$$\bar{w}_{AB}''(L_1) = w''_{BC}(0): \quad B_2 = A_1 \sin \lambda L_1 \quad (3-74)$$

$$\bar{w}_{BC}(0) = 0: \quad B_2 + D_2 = 0; \rightarrow D_2 = -B_2 \quad (3-75)$$

$$\begin{aligned} \bar{w}_{BC}(b) = \bar{w}_{CD}(0): \\ A_1 \sin \lambda L_1 [\cos \lambda b - \cosh \lambda b] + A_2 \sin \lambda b + C_2 \sinh \lambda b - B_3 - D_3 = 0 \end{aligned} \quad (3-76)$$

$$\bar{w}'_{BC}(b) = \bar{w}'_{CD}(0):$$

$$-A_1 \sin \lambda L_1 [\sin \lambda b + \sinh \lambda b] + A_2 \cos \lambda b - A_3 + C_2 \cosh \lambda b - C_3 = 0 \quad (3-77)$$

$$\bar{w}_{BC}''(b) = \bar{w}_{CD}''(0):$$

$$-A_1 \sin \lambda L_1 [\cos \lambda b + \cosh \lambda b] - A_2 \sin \lambda b + B_3 + C_2 \sinh \lambda b + -D_3 = 0 \quad (3-78)$$

$$\bar{v}_{HG}(0) = 0; \rightarrow Q_1 = 0: \rightarrow \bar{v}_{HG} = P_1 \sin \gamma x_c \quad (3-79)$$

$$\bar{w}_{CD}'''(0, t) - \bar{w}_{BC}'''(b, t) = \frac{-c[\dot{w}_{BC}(b) - \dot{v}(a)]}{EI} :$$

$$-A_3 + C_3 - [-A_2 \cos \lambda b + A_1 \sin \lambda L_1 [\sin \lambda b - \sinh \lambda b] + C_2 \cosh \lambda b] = -i\eta [A_2 \sin \lambda b + B_2 \cos \lambda b + C_2 \sinh \lambda b + D_2 \cosh \lambda b - P_1 \sin \gamma a$$

Substituting $B_2 = -D_2 = A_1 \sin \lambda L_1$ into the above equation

$$A_1 \sin \lambda L_1 [\sinh \lambda b - \sin \lambda b + i\eta (\cos \lambda b - \cosh \lambda b) + A_2 \cos \lambda b + i\eta \sin \lambda b - A_3 + C_2 i\eta \sinh \lambda b - \cosh \lambda b + C_3 - i\eta P_1 \sin \gamma a = 0 \quad (3-80)$$

where $\eta = C_0 \omega / (\lambda^3 EI)$ (3-81)

$$\bar{w}_{CD}(b') = \bar{w}_{ED}(L_4):$$

$$A_3 \sin \lambda b' - A_4 \sin \lambda L_4 - A_5 \sin \lambda L_3 [\cos \lambda L_4 - \cosh \lambda L_4] + B_3 \cos \lambda b' + C_3 \sinh \lambda b' - C_4 \sinh \lambda L_4 + D_3 \cosh \lambda b' = 0 \quad (3-82)$$

$$\bar{w}'_{CD}(b') = -\bar{w}'_{ED}(L_4):$$

$$A_3 \cos \lambda b' + A_4 \cos \lambda L_4 - A_5 \sin \lambda L_3 [\sin \lambda L_4 + \sinh \lambda L_4] - B_3 \sin \lambda b' + C_3 \cosh \lambda b' + C_4 \cosh \lambda L_4 + D_3 \sinh \lambda b' = 0 \quad (3-83)$$

$$\bar{w}_{CD}''(b') = \bar{w}_{ED}''(L_4):$$

$$-A_3 \sin \lambda b' + A_4 \sin \lambda L_4 + A_5 \sin \lambda L_3 [\cos \lambda L_4 + \cosh \lambda L_4] - B_3 \cos \lambda b' + C_3 \sinh \lambda b' - C_4 \sinh \lambda L_4 + D_3 \cosh \lambda b' = 0 \quad (3-84)$$

$$EI w_{CD}'''(b', t) + EI w_{ED}'''(L_4, t) = -T \cos \theta \frac{\partial v_{DG}(0, t)}{\partial x}:$$

$$-A_3 \cos \lambda b' - A_4 \cos \lambda L_4 + A_5 \sin \lambda L_3 [\sin \lambda L_4 - \sinh \lambda L_4] + B_3 \sin \lambda b' + C_3 \cosh \lambda b' + C_4 \cosh \lambda L_4 + D_3 \sinh \lambda b' + P_2 \frac{\gamma T \cos \theta}{\lambda^3 EI} = 0 \quad (3-85)$$

$$\bar{w}'_{FE}(L_3) = \bar{w}'_{ED}(0): \quad A_4 - A_5 \left[\cos \lambda L_3 - \frac{\sin \lambda L_3}{\sinh \lambda L_3} \cosh \lambda L_3 \right] + C_4 = 0 \quad (3-86)$$

$$v_{HG}(a) = v_{DG}(a'): \quad P_1 \sin(\gamma a) - P_2 \sin(\gamma a') - Q_2 \cos(\gamma a') = 0$$

From which

$$Q_2 = P_1 \frac{\sin(\gamma a)}{\cos(\gamma a')} - P_2 \frac{\sin(\gamma a')}{\cos(\gamma a')} \quad (3-87)$$

$$v_{DG}(0) = w_{CD}(b'):$$

$$A_3 \sin \lambda b' + B_3 \cos \lambda b' + C_3 \sinh \lambda b' + D_3 \cosh \lambda b' - Q_2 = 0 \quad (3-88)$$

Substituting Eq. (3-87) into Eq. (3-88) gives

$$A_3 \sin \lambda b' + B_3 \cos \lambda b' + C_3 \sinh \lambda b' + D_3 \cosh \lambda b' - P_1 \frac{\sin(\gamma a)}{\cos(\gamma a')} + P_2 \frac{\sin(\gamma a')}{\cos(\gamma a')} = 0 \quad (3-89)$$

$$T \cos \theta \left\{ \left[\frac{\partial v(x, t)}{\partial x} \right]_{a^+} - \left[\frac{\partial v(x, t)}{\partial x} \right]_{a^-} \right\} = C_0 \left\{ \frac{dv(a, t)}{dt} - \frac{dw(b, t)}{dt} \right\}$$

→

$$T \cos \theta \left\{ - \left[\frac{\partial \bar{v}_{DG}}{\partial x} \right]_{a'} - \left[\frac{\partial \bar{v}_{HG}}{\partial x} \right]_a \right\} e^{i\omega t} = C_0 \{ \bar{v}_{HG}(a) i\omega e^{i\omega t} - \bar{w}_{CD}(0) i\omega e^{i\omega t} \}$$

$$\rightarrow T \cos \theta \{ -(P_2 \gamma \cos \gamma a' - Q_2 \gamma \sin \gamma a') - P_1 \gamma \cos \gamma a \} = C_0 \{ P_1 \sin \gamma a - (B_3 + D_3) \} i\omega$$

$$i\beta B_3 + i\beta D_3 - P_1 (i\beta \sin \gamma a + \cos \gamma a) - P_2 \cos \gamma a' + Q_2 \sin \gamma a' = 0 \quad (3-90)$$

$$\text{where } \beta = \frac{C_0 \omega}{\gamma T \cos \theta} \quad (3-91)$$

Substituting Eq. (3-87) into Eq. (3-90) gives

$$i\beta B_3 + i\beta D_3 - P_1 (i\beta \sin \gamma a + \cos \gamma a - \tan \gamma a' * \sin \gamma a) - P_2 (\cos \gamma a' + \tan \gamma a' \sin \gamma a) = 0 \quad (3-92)$$

Equations (3-73),(3-76), (3-77),(3-78), (3-80),(3-82), (3-83),(3-84), (3-85),(3-86), (3-89) and (3-92) can be combined into

$$[G]\{S\} = \{0\} \quad (3-93)$$

where $\{0\}$ is a 12x1 null matrix, $\{S\} = \{A_1 A_2 A_3 A_4 A_5 B_3 C_2 C_3 C_4 D_3 P_1 P_2\}'$ is a 12x1 matrix containing the unknown constants for describing the shape functions and $[G]$ is a 12x12 matrix as follows.

$$G = \begin{bmatrix} G11 & G12 & G13 & G14 \\ G21 & G22 & G23 & G24 \\ G31 & G32 & G33 & G34 \\ G41 & G42 & G43 & G44 \end{bmatrix}$$

The 3X3 sub matrices are as follows

$$G11 = \begin{bmatrix} C1 - (CHT1)(S1) & -1 & 0 \\ S1(Cb - CHb) & Sb & 0 \\ -S1(Sb + SHb) & Cb & -1 \end{bmatrix}$$

$$G12 = \begin{bmatrix} 0 & 0 & 0 \\ 0 & 0 & -1 \\ 0 & 0 & 0 \end{bmatrix}$$

$$G13 = \begin{bmatrix} -1 & 0 & 0 \\ SHb & 0 & 0 \\ CHb & -1 & 0 \end{bmatrix}$$

$$G14 = \begin{bmatrix} 0 & 0 & 0 \\ -1 & 0 & 0 \\ 0 & 0 & 0 \end{bmatrix}$$

$$G21 = \begin{bmatrix} -S1(Cb + CHb) & -Sb & 0 \\ S1(SHb + i\eta Cb - Sb - i\eta CHb) & Cb + i\eta Sb & -1 \\ 0 & 0 & Sb' \end{bmatrix}$$

$$G22 = \begin{bmatrix} 0 & 0 & 1 \\ 0 & 0 & 0 \\ -S4 & -S3(C4 - Ch4) & -Cb' \end{bmatrix}$$

$$G23 = \begin{bmatrix} Sb & 0 & 0 \\ -CHb + i\eta Sb & 1 & 0 \\ 0 & Sb' & -S4 \end{bmatrix}$$

$$G24 = \begin{bmatrix} -1 & 0 & 0 \\ 0 & -i\eta SGa & 0 \\ CHb' & 0 & 0 \end{bmatrix}$$

$$G31 = \begin{bmatrix} 0 & 0 & Cb' \\ 0 & 0 & -Sb' \\ 0 & 0 & Cb' \end{bmatrix}$$

$$G32 = \begin{bmatrix} C4 & -S3(S4 + SH4) & -Sb' \\ S4 & S3(C4 + CH4) & -Cb' \\ -C4 & S3(S4 \pm SH4) & Sb' \end{bmatrix}$$

$$G33 = \begin{bmatrix} 0 & CHb' & CH4 \\ 0 & SHb' & -SH4 \\ 0 & CHb' & C4 \end{bmatrix}$$

$$G34 = \begin{bmatrix} SHb' & 0 & 0 \\ CHb' & 0 & 0 \\ SHb' & 0 & \gamma T \cos\theta / (\lambda^3 EI) \end{bmatrix}$$

$$G41 = \begin{bmatrix} 0 & 0 & 0 \\ 0 & 0 & Sb' \\ 0 & 0 & 0 \end{bmatrix}$$

$$G42 = \begin{bmatrix} 1 & -C3 + (S3)(CH3)/SH3 & 0 \\ 0 & 0 & Cb' \\ 0 & 0 & i\beta \end{bmatrix}$$

$$G43 = \begin{bmatrix} 0 & 0 & 1 \\ 0 & SHb' & 0 \\ 0 & 0 & 0 \end{bmatrix}$$

$$G_{44} = \begin{bmatrix} 0 & 0 & 0 \\ Cb' & -SGa/CGa' & TGa' \\ i\beta & -i\beta(SGa) - CGa - (TGa') * SGa & -CGa' - (TGa')(SGa') \end{bmatrix}$$

where $Ci = \cos\lambda L_i, i = 1,2,3,4., CHi = \cosh\lambda L_i, i = 1,2,3,4., Cb = \cos\lambda b, Cb' = \cos\lambda b', CGa = \cos\gamma a, CGa' = \cos\gamma a', Si = \sin\lambda L_i, i = 1,2,3,4., SHi = \sinh\lambda L_i, i = 1,2,3,4., Sb = \sin\lambda b, Sb' = \sin\lambda b', SGa = \sin\gamma a, \text{ and } SGa' = \sin\gamma a'.$

3.4 Solution to equation of motion

The nontrivial solution of Eq.(3-93) requires to satisfy Eq. (3-94) which will lead to the characteristic equation of motion of coupled system. The solution to the characteristic equation will be the complex eigen frequencies corresponding to different modes of damped free vibration of the system.

$$\det|G| = 0 \tag{3-94}$$

The characteristic equation contains the mass density m_2 and the bending stiffness EI of the equivalent beam. They can be derived based on the following two conditions.

- Static condition: Vertical static deflection at cable-deck anchorage point is zero.
- Dynamic condition: 1st symmetric vertical bending frequency of the three-span continuous beam is consistent with that of the original bridge super structure.

The detailed derivations for determining m_2 and EI are given in the Appendix A and Appendix B.

3.4.1 Conversion of parameters and trigonometric functions into linear terms

The characteristic equation of the cable-damper-deck coupled system contains parameters λ and η which have nonlinear relationships with frequency ω . Also it has trigonometric and hyperbolic expressions which contain nonlinear terms of ω . As seen from the Taylor's expansion, the higher order derivatives of these parameters and functions with respect to the frequency ω is not significant. Hence, these functions are converted to linear functions of ω using Taylor's expansion with the base value as the 1st modal frequency of the cable, ω_0 . This conversion is carried out in the current analysis using a Matlab program. Parameters λ in Eq. (3-68) and η in Eq. (3-81) are converted to linear functions of ω as follows:

$$\lambda = \omega_0^{\frac{1}{2}} \sqrt{m_2/EI} + \frac{1}{2} \omega_0^{-\frac{1}{2}} \sqrt{m_2/EI} (\omega - \omega_0) \quad (3-95)$$

$$\eta = \frac{C_0}{EI} \left(\frac{EI}{m_2}\right)^{\frac{3}{4}} \omega_0^{-\frac{1}{2}} - \frac{C_0}{EI} \left(\frac{EI}{m_2}\right)^{\frac{3}{4}} \omega_0^{-\frac{3}{2}} (\omega - \omega_0) \quad (3-96)$$

3.4.2 Relation between solution and damping ratio

The characteristic equation of the coupled system comprises a matrix [G], which is a 12x12 matrix. Therefore, in general, the solution will yield 12 complex eigenvalues. The magnitude of the correct solution should be the first modal frequency of cable ω_0 from which the accuracy of calculation could be verified and the imaginary part will represent $\xi \omega_0$, from which the damping ratio ξ of the cable could be obtained.

3.4.3 Analysis Procedures

As described in section 3.3, the simplified equivalent system consists of three main components: a three-span equivalent continuous beam which represent the bridge deck and all the supporting cables except the cable considered in the analysis, a stay cable and a damper. The solution to the equation of motion of the coupled cable-damper-deck system are the roots of its characteristic equation, Eq.(3-94). A Matlab program was developed to solve this equation. The input data (please refer to Fig.3-5) include the cable tension(T); the mass density of the cable(m_1); the length of the cable (L); the fundamental frequency of the cable (f_0); the horizontal distance from the pylon end to the damper location of the cable (a); the horizontal distance from the bridge deck end to the damper location of the cable (a'); the damping coefficient of the damper (C); the angle of inclination of the cable (θ); and the first vertical bending frequency of cable–deck system(f_s).

The analysis procedures are as follows:

- Step 1- Calculation of mass density m_2 and bending stiffness EI of the three-span continuous equivalent beam.
 - a) Use the static condition in Appendix A to get the relationship between m_2 and EI .
 - b) Apply the dynamic condition in Appendix B to converge the frequency of the first vertical global bending mode of the equivalent beam to f_s by varying the cross section of the equivalent beam.
 - c) Now check if the static condition is still satisfied. If not, then vary the density of the equivalent beam material ρ_s to obtain zero deflection at the cable-deck

anchorage. Apply new EI and m_2 in b). Repeat a) to c) until both static and dynamic conditions are satisfied.

- Step-2- Use Taylor expansion with the base value of $\omega_0 = 2\pi f_0$ to convert all parameters, trigonometric and hyperbolic functions in matrix $[G]$ into linear terms of ω . Then solve matrix $[G]$ to obtain eigen frequencies. A Matlab program was developed to perform these tasks.

- Step-3- The solution will be in the form $\alpha + i\beta$, where both α and β are positive values

$$\text{and } \omega_0 = \sqrt{\alpha^2 + \beta^2}, \zeta = \frac{\beta}{\sqrt{\alpha^2 + \beta^2}}.$$

CHAPTER IV CASE STUDY

A case study of cable vibration control on a real cable-stayed bridge, the Sutong bridge in China, is presented in this chapter. The impact of deck vibration on the efficiency of the external damper is studied using the proposed model and method described in chapter 3. Results will be compared with those from other studies.

4.1 Description of the example bridge

The Sutong bridge is at present the world's largest cable-stayed bridge, situated in Jiangsu province, China. It provides the transportation and economical link between Suzhou and Nantang crossing the Yangtze river. The key issues related to this bridge are significant ship traffic (over 2000 ships per day), high design wind speed, strong currents, poor soil conditions, 306 m high concrete pylons and a record main span. A photograph of the bridge is shown in Fig.4-1.

The bridge is a double cable plane, twin-pylon cable-stayed bridge with a continuous span arrangement of 2,088 m as shown in Fig.4-2. Two auxiliary piers and one transitional pier are erected in each side span. The main span of the bridge is 1088m, which is the longest main cable-stayed bridge span at present.

The bridge girder is a streamlined closed flat steel box girder. The total width including wind fairing is 41.0 m accommodating dual 8 traffic lanes. The cross section height is 4.0m. The steel box is generally stiffened in the longitudinal direction with closed steel troughs. Transverse plate diaphragms are provided with a typical distance of 4.0m and with smaller distances down to 2.27 m locally around the two pylons.

The inverted Y-shaped pylons are about 300m in height and are made of concrete grade C50 according to the Chinese standard JTJ01-89. The stay cables are anchored inside steel boxes fixed to the concrete by shear studs at the pylon top. The stay cables are arranged in double inclined cable planes with standard spacing of 16m in the central span and 12m near the ends of the back span along the girder. To reduce the effect of wind loads, the cable stay systems are made of the parallel wire strand consisting of 7mm wires, each with a cross sectional area of 38.48mm^2 . The nominal tensile strength of cables is 1770MPa. The longest cable is about 577m with a weight of 59 tons.

The bridge has total of 272 stay cables. The longest 48 stay cables are damped with semi-active magneto-rheological (MR) dampers. These dampers consists quite conventionally of a cylinder, a piston and a fluid. The fluid is magnetic and its shear strength, that is, its viscosity can be controlled by the surrounding magnetic field. By controlling the currents that create the magnetic field the resistance with which the damper reacts to the respective vibration can be controlled. Another 152 cables are equipped with linear viscous passive dampers. These dampers are preset to a certain response force that is a compromise of the total system. A typical linear viscous damper is shown in Fig. 4-3.

It is intended to estimate the damping ratio of a typical stay cable near the mid span of the Sutong bridge by considering the cable-deck interaction using the proposed model and method.



Figure 4-1 Sutong bridge –Jiangsu Province ,China

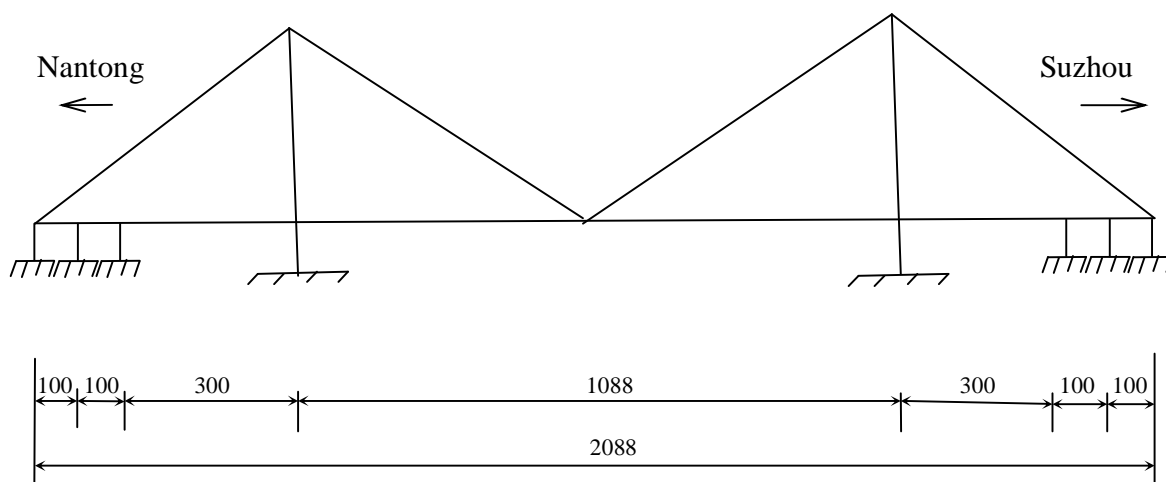


Figure 4-2 Schematic diagram of span arrangements with only outermost cables in Sutong bridge (unit m)



Figure 4-3 A viscous damper attached to a bridge stay cable

4.2 Effectiveness of damper by considering the cable-deck interaction

In the current analysis, the bridge is idealized as an equivalent three-span continuous beam with span arrangement of (300 + 1088 + 300) m. The equivalent beam represents the behaviour of the original bridge girder and all the stay cables except the studied one in the mid-span. The stay cable investigated in the model is the longest stay cable at mid-span at Nantong end. Though on the bridge site, MR damper is used for the longest cable, no matured model has been developed to simulate the behavior of the MR damper. Since a linear viscous damper is included in the proposed cable-damper-deck model, and many studies have been performed considering a cable equipped with a linear viscous damper, this case study also assumed a linear viscous damper is attached to the longest cable. The passive damper connects to the stay cable close to the cable anchorage point on the bridge deck. The numerical model of the cable-damper-deck system is shown schematically in Fig. 4-4.

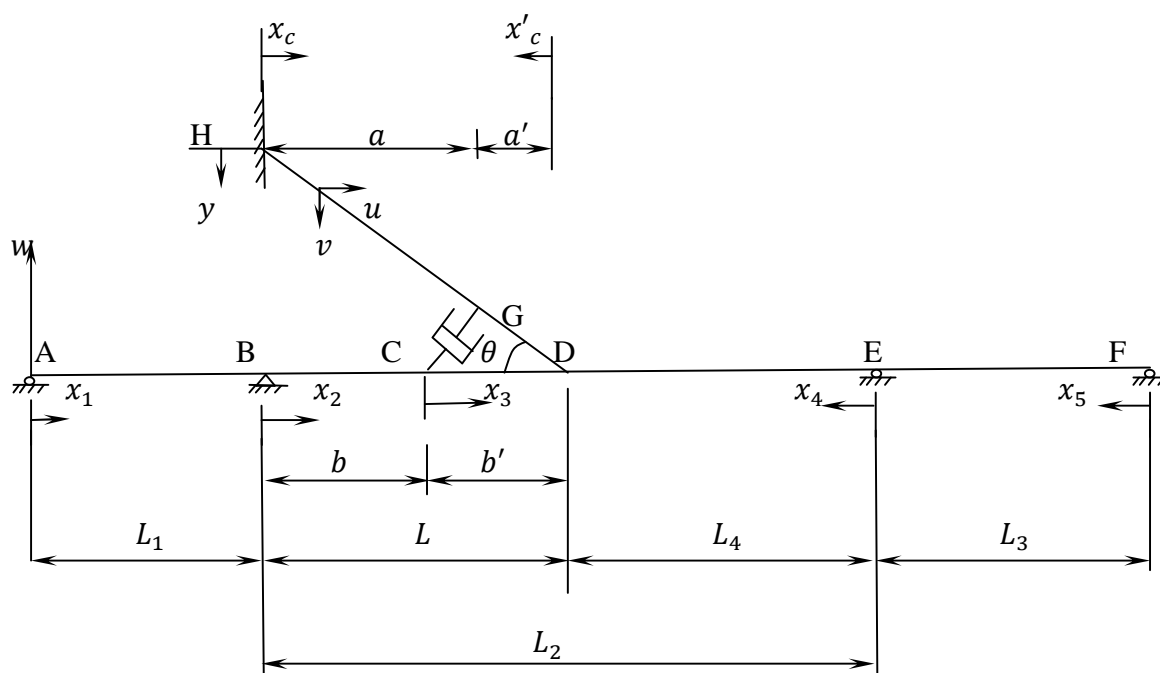


Figure 4-4 Typical cable-damper-deck coupled model

The physical and dynamic properties of the cable and the damper are listed in Table 4-1. In the given data, T is the static tension of the cable in kN, m_1 is the unit mass of the cable in kg/m length, L is the horizontal projected length of the cable, f_0 is the natural frequency of the cable, a is the horizontal distance from cable-damper contact point to the pylon, a' is the from cable-deck anchorage point to the cable-damper contact point, C_0 is the coefficient of damper, θ is the angle of inclination of the cable and f_s is the fundamental frequency of the bridge.

Table 4-1 The main parameters of the longest cable and damper

T (kN)	m_1 (kg/m)	L (m)	f_0 (Hz)	a (m)	a' (m)	C_0 (kNs/m)	θ (deg)	f_s (Hz)
6708	100.8	532.925	0.224	526.139	6.785	325	22.46	0.195

Detailed analysis is shown below.

1. ABAQUS model is created using the following data (please refer to Fig. B-1 in Appendix B)

$$\begin{aligned}
 L &= 532.975m & E_s &= 2.0 \times 10^{11} N/m^2 \\
 L_1 &= 300m & E_c &= 7.0 \times 10^{10} N/m^2 \\
 L_2 &= 1088m & R_c &= 0.065m \\
 L_3 &= 300m & \text{Initial stress of cable} &= 5.053 \times 10^8 N/m^2 \\
 h &= L \tan(22.46) & \rho_c &= 2400 kg/m^3 \\
 T &= 6708000 N \\
 \rho_s &= 7850 kg/m^3
 \end{aligned}$$

where E_s is the modulus of elasticity of steel, E_c is the modulus of elasticity of material of the equivalent beam, R_c is the radius of the stay cable, ρ_s is the density of steel and ρ_c is the density of the equivalent beam material.

2. Select a rectangular hollow section for the equivalent beam. Use width = 32m , height $d = 5m$ and thickness $t = 0.18m$ as the initial values.
3. Adjust the ρ_c value so that static deflection at the cable-deck anchorage point is zero (condition given in Appendix A).
4. Run the ABAQUS program to get the 1st vertical bending frequency f_s of the cable-deck system.
5. If the frequency f_s does not equal to the 1st vertical bending frequency of the original bridge (0.195 Hz), change the height of the beam section used in Step 2 above and repeat Steps 3 & 4 until f_s converges to 0.195Hz.

6. Calculate unit mass m_2 of the equivalent beam using

$$m_2 = \rho_c (bd - (b - 2t)(d - 2t)), \text{ where } b, d \text{ and } t \text{ are obtained in Step 5.}$$

7. The final EI and m_2 values thus obtained are used in Eq. (3-94). This equation is solved using Matlab to obtain damping ratio of the cable as described below. The corresponding Matlab source code is given in Appendix E.

Results of the above calculation in the current example:

$$EI = 3.45 \times 10^{11} \text{ N}\cdot\text{m}^2 \text{ and } m_2 = 264.58 \text{ kg/m}$$

Table 4-2 Input parameters in matrix G

a'	6.785 m	L	532.925 m
θ	0.392 rad.	L_1	300 m
m_1	100.8 kg/m	L_3	300 m
m_2	264.58 kg/m	L_4	555.075 m
T	6708000 N	C_0	325000 N·s/m
EI	$3.45 \times 10^{11} \text{ N}\cdot\text{m}^2$		

All the elements in matrix [G] can be obtained using the input parameters listed in Table 4-2. These elements are then converted to linear terms of ω using Taylor's expansion as described in Section 3.4.3, with the base value of frequency $\omega_0 = 2\pi f_0 = 1.407 \text{ rad/sec}$. The determinant of the final matrix [G] is an 11th order polynomial of ω . The following roots can be obtained with the formulation of ω in linear terms.

1.524239221+0.1132960e-2i	-20660.071092437+2303.751704748i
1.459476458+0.3771170e-2i	-27.811067728+1.953496478i
0.561176513+0.25974130e-1i	-5.657006310-0.28546957e-1i
9.693705852+3.306724103i	-42.560825603-50.072125598i
0.832321640+1.169200114i	0.524634081-0.109495838i
0.14029283e-1+2.717521802i	

Root selection was done based on the expression of the complex eigen-frequency at $\omega = \sqrt{1 - \zeta^2} \omega_0 + i\zeta \omega_0$ where both real and imaginary parts of the correct root should be positive. Out of these selected roots, the one with the value closest to $\omega_0 = 1.407 \text{ rad/sec}$ is $1.459476458 + 0.3771170e - 2i$. The circular frequency corresponding to this root is $\omega = \sqrt{1.45947^2 + 0.003771^2} = 1.459 \text{ rad/s}$ and the damping ratio is $\zeta = \frac{0.003771}{1.459} = 0.00258$.

4.3 Comparison with other models

4.3.1 Fixed-fixed cable model

Theoretical derivation given in Appendix C can be used to obtain the damping ratio of the cable fixed at both ends. The Matlab source code along with the cable and the damper input data for the above example given in Appendix F yields: $\omega = 1.408 + 0.0072i$ and hence damping ratio $\xi = 0.0051$.

4.3.2 Cantilever beam model by Liang et al (2008)

The model proposed by Liang et al (2008) to investigate the effect of cable-deck interaction on the damper performance is adopted here to compare the results from the current model. In Liang's model, the bridge girder is idealized as a cantilever beam supported at the

pylon. A schematic diagram of the model is shown in Fig. 4-5. The damping ratio obtained using this model yields a cable damping ratio of $\zeta = 0.00153$ when the damper is installed.

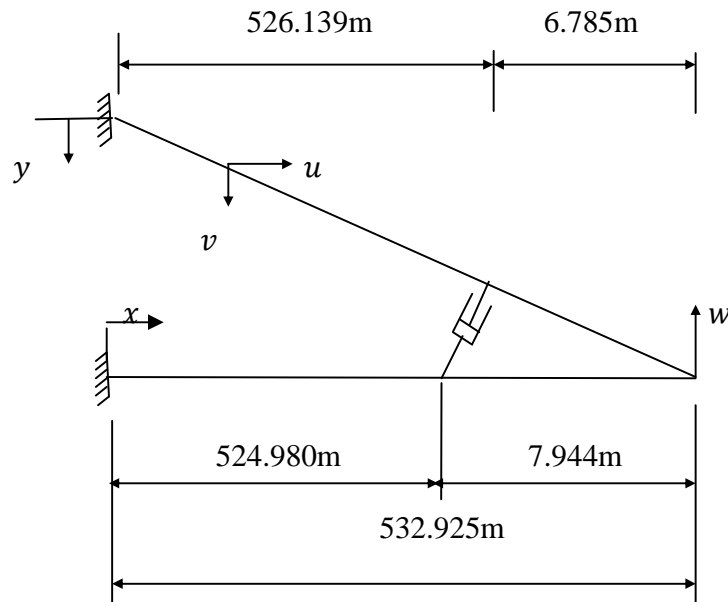


Figure 4-5 Simplified cantilever beam model used by Liang et al (2008)

Besides, the fixed-fixed cable scenario can be considered as a special case when Eq.(3-94) is applied. It was assumed that the equivalent continuous beam is very rigid by substituting an EI value two orders higher than the derived value ($EI = 3.45 \times 10^{11} \text{N} \cdot \text{m}^2$) into Eq.(3-94) while keeping the rest of the input data unchanged. This would allow to simulate a no deck vibration scenario. This yields $\omega = 1.403 \text{ rad/sec}$ and a damping ratio $\xi = 0.0051$.

Results of the damping ratio of the longest cable on Sutong bridge after attaching to a damper and predicted by using different models and approaches are summarized in Table 4-3. The analysis of cable fixed-fixed support condition using the theoretical approach and the proposed model with rigid bridge girder yields the same equivalent cable damping ratio. This verifies the validity of the proposed equivalent 3-span continuous beam model. Both the

cantilever beam model used by Liang et al (2008) and the proposed 3-span continuous beam model which considers the cable-deck interaction in the analysis yield a damping ratio considerably less than that of the fixed-fixed cable case. Hence, the available design curve and formulae for selecting optimum damper, which are based on the assumption that the cable is fixed at both ends might be too optimistic.

Table 4-3 Summary of results

Model	Root of the characteristic equation, ω	Damping ratio ζ
Fixed-fixed cable (Theoretical derivation)	$1.408 + 0.0072i$	0.0051
Fixed-fixed cable (Proposed equivalent 3-span cantilever beam model)	$1.403 + 0.00712i$	0.0051
Cantilever beam model Liang et al(2008)	—	0.00153
Proposed equivalent 3-span cantilever beam model. (consider deck vibration)	$1.459 + 0.00377i$	0.00258

The above set of results suggests that in the case of a flexible long-span cable-stayed bridge, the consideration of cable-deck interaction in assessing the effectiveness of an external damper in cable vibration control is necessary. For the Sutong bridge studied here, the locations of the cable anchorage point and the damper support on the deck are almost 8 m apart. Displacements and velocities at these two locations are highly dependent on the deformation shape of the bridge girder. In the case of a linear viscous damper, the actual damping force is

proportional to the relative velocity between the cable-damper attaching point and the deck-damper anchorage point. Hence, the bridge girder motion would affect the amount of damping offered by the damper to the stay cable.

In the cantilever beam model by Liang et al (2008), the bridge girder is simplified as a cantilever beam with one end fixed at the pylon. Compared to a typical double tower bridge, of which the main portion consists of two side spans and one main span, the cantilever assumption would alter the response characteristics of the actual bridge girder due to inconsistent boundary conditions. Therefore, the motion at the cable-deck and the damper-deck connections and their relations cannot be correctly represented. The impact of deck vibration on the efficiency of the damper yielded from such a model could be misleading.

The three-span continuous beam model proposed in the current study has the advantage that the boundary conditions are kept consistent with the actual bridge girder. The girder deformation and the mode shapes can thus be well simulated. It is worth mentioning that the same model and approach proposed in this study can be applied to obtain damping characteristics for higher modes of cable vibrations. In the analysis of higher modes, the corresponding modal frequency of the cable should be used as the base value in the Taylor's expression.

4.4 Other Case studies

The objective of considering other case studies is to investigate the effect of cable-deck interaction on the damper efficiency and its impact on cable-stayed bridges with different span lengths. Four medium to long-span cable-stayed bridges with main span ranging from 432m to 1018m were selected in this set of analyses. All the bridge data and input parameters relevant to the analyses are given in Table 4-4 and Table 4-5, respectively, and described in Fig.4-4.

4.4.1 Description of bridges used in the case studies

4.4.1.1 Stonecutters Bridge – Hong Kong, China

The Stonecutters bridge is a long-span cable stayed bridge carrying dual 3 lane highway over Rambler Channel at the entrance to the Kwai Chung container port in Hong Kong. The bridge main span has a twin deck cross-section with a length of 1018m. The twin decks are connected at intervals by transverse steel box girders. The two single



Figure 4-6 View of Stonecutters bridge at the entrance to the Kwai Chung container port

leg pylons are 290m tall with a lower section in concrete and the upper section formed in composite steel/concrete. The bridge also includes 4-span twin deck concrete side spans of total length of 289 m on each side. These 4-spans are treated in dynamic analysis of the present study as a single span. Hence the span configuration of the 3-span equivalent continuous beam is 289 m + 1018 m + 289 m.

The circular tapered mono-column towers stand on the bridge centre line between the two longitudinal box girders of the twin girder deck. Stay cables are in two planes arranged in a

modified fan layout and attached with the outside edges of the deck girders. The deck girders are connected with cross girders spaced at 18 m in the main span coinciding with the stay anchorage spacing and 20 m in the back spans where the stays anchorages are spaced at 10 m. The length of the longest stay cable is 540 m and the weight is 75 tons. The first vertical bending frequency of the bridge is 0.244 Hz.

4.4.1.2 Tatara Bridge – Japan



Figure 4-7 Tatara Bridge

The Tatara bridge is a cable-stayed bridge measuring 1480m in total length which links Ikuchijima Island and Hiroshima Prefecture in Japan. The main girder section consists of 3 spans, 270 m, 890 m and 320 m. As either side span is shorter than the center span, PC girders are installed at each end of both the side span sections as counterweight girders to resist negative reaction. This cable-stayed bridge thus uses a steel and PC connection girder. The main tower is 220m high and designed as an inverted Y shape. Cables are installed at 21 levels in two planes with multi-fan pattern. The length of the longest cable is 460 m and it has a mass density of 122 kg/m.

The width of the bridge is 30.6 m including the sidewalk. The girder height is 2.7 m and it uses flat box girders attached with fairings to ensure wind stability. The first vertical bending frequency of the bridge is 0.199 Hz.

4.4.1.3 Third Nanjing Yangtze Bridge - China



Figure 4-8 Third Nanjing Yangtze Bridge

The third Nanjing Yangtze bridge is a 5-span cable-stayed bridge with two towers. The bridge is situated on the road between Shanghai and Chengdu in Jiangsu province in China. The span arrangement is 63 m + 257 m + 648 m + 257 m + 63 m. In the present analysis, the bridge is treated as a 3-span continuous beam by considering the span arrangement as 257 m + 648 m + 257 m.

The streamlined steel box girder deck has an overall width of 37.2 m and a structural height of 3.2 m. The deck facilitates 3 lane dual traffic and is designed for a vehicular speed of 100 km/h. The two steel towers with a height of 215 m resemble a curved narrow “A” shape

when seen along the bridge. The towers are made up of concrete from the foundation up to the deck level and the portion above the deck level is of steel. The stay cables are arranged in two inclined planes in a modified- fan layout with the longest cable being 354.5 m in length and has a mass density of 72.1 kg/m. The first vertical bending frequency of the bridge is 0.243 Hz.

4.4.1.4 Donghai Bridge - China



Figure 4-9 Donghai Bridge

Donghai bridge is one of the longest cross-sea bridges in the world. It has a total length of 32.5 km and connects mainland Shanghai and the offshore Yangshan deepwater port in China. The cable-stayed section of the bridge has the longest span of 420 m, in order to allow for the passage of large ships. It has a navigation capacity of 5000 tons and a navigation height of 40 m.

The bridge is a five-span continuous cable-stayed bridge with double pylons, single cable plane and auxiliary piers. The span arrangement is 73 m + 132 m + 420 m + 132 m + 73 m. In the present study it is treated as a three-span continuous beam by considering only the middle 3 spans. The bridge is designed according to the two-way six-lane expressway standard and the deck is 33 m wide.

The pylon section above the deck has inverted Y shape while that below the deck is a box structure with uneven width. The 4.0m deep main girder has a steel-concrete composite of single-box-three-cell section. The top plate of the box girder is 33.0 m wide with two 4.5 m wide cantilevers. The standard cable spacing is 8m on the girders and 2.2 m on the pylons, totalling 224 cables overall. The length of the longest stay cable is 227 m and its mass density is 85.3 kg/m. The first vertical bending frequency of the bridge is 0.388 Hz.

Table 4-4 Summary of bridge data

Bridge	Sutong (Liang et al, 2008)	Stonecutters (Vijrum et al 2006)	Tatara (Yabuno et al 2003)	Nangjing (Liang et al, 2008)	Donghai (Liang et al, 2008)
L_1 (m)	300	289	270	255	132
L_2 (m)	1088	1018	890	648	432
L_3 (m)	300	289	320	255	132
L (m)	532.925	496.330	422.680	315.297	203.876
θ (rad)	0.392	0.405	0.405	0.475	0.455
a' (m)	6.785	9.430	5.280	4.015	2.596
b' (m)	7.944	11.160	6.260	5.077	3.217
Cable tension T (kN)	6708	7000	6714	3785	5723
Radius of cable R_c (m)	0.065	0.064	0.0702	0.054	0.06
Natural frequency of cable f_c (Hz)	0.224	0.244	0.255	0.323	0.571
Frequency of 1 st global vertical mode of the bridge f_s (Hz)	0.195	0.26	0.199	0.243	0.388
Damper capacity C (N·s/m)	325000	332000	357717	206000	276000

Table 4-5 Summary of equivalent beam data

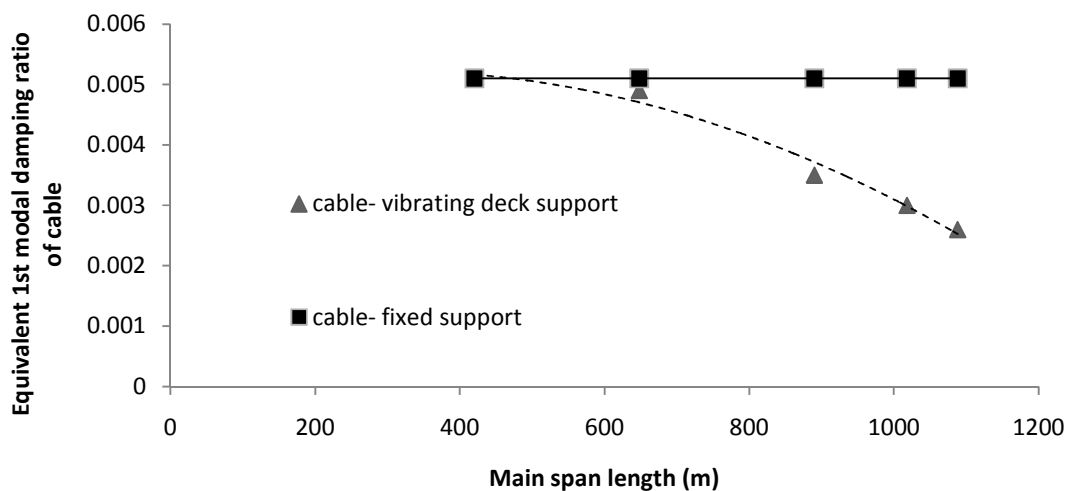
Bridge	Sutong	Stonecutters	Tatara	Nanjing	Donghai
Cross-section of the equivalent beam (hollow box section) width x depth x thickness	32x6x0.18	32x11x0.3	32x8.2x0.2	32x12.4x0.25	34x4.34x0.2
Modulus of elasticity of equivalent beam E_b (N/m ²)	3×10^9	1×10^9	1×10^9	1×10^8	1.1×10^9
Bending stiffness of equivalent beam EI (N·m ²)	3.45×10^{11}	6.06×10^{11}	1.5×10^{11}	6.61×10^{10}	6.64×10^{10}
Density of equivalent beam material ρ_c (kg/m ³)	17.65	11.8	20.95	10.95	41.7
Mass density of equivalent beam m_2 (kg/m)	264.58	300.192	322.38	240.35	632.83

The bending stiffness EI of the equivalent beam and the mass density m_2 of the equivalent beam obtained above are then used in Eq. (3-94) to determine the acceptable root of the characteristic equation and to find the damping ratio of the selected cable of each bridge as described in Section 3.4.3 Steps 2-4. For comparison, damping ratios are also calculated for the cable fixed-fixed condition for each bridge based on the theoretical derivation. The input source code of Matlab program for these calculations is provided in Appendix E. The results are summarized in Table 4-6 below.

Table 4-6 Summary of case study results

Bridge	Main span length (m)	Proposed model (consider deck vibration)		Analytical model of fixed-fixed cable (Appendix C)		% Difference*
		ω	ξ	ω	ξ	
Sutong	1088	1.459+0.0038i	0.0026	1.408+0.0072i	0.0051	49
Stonecutters	1018	1.604+0.0048i	0.0030	1.537+0.0077i	0.0050	40
Tatara	890	1.683+0.0059i	0.0035	1.606+0.0080i	0.0050	30
Nangjing	648	2.081+0.0101i	0.0049	2.035+0.0104i	0.0051	4
Donghai	432	3.621+0.0186i	0.0051	3.594+0.0185i	0.0051	0

*Used cable fixed-fixed condition as reference

Figure 4-10 Equivalent 1st modal damping ratio of cable vs main span length

The five cable-stayed bridges, including Sutong bridge and the other four in the case studies, with main span length varying from 432m to 1088m, covered the range of medium- to long-span cable-stayed bridges quite well. Though different proportions of adjacent span lengths affect the mode shape and frequency of vibration, and the location of the damper on the bridge girder also influences the relative speed of the damper with respect to the cable and hence the damping force, the results clearly indicate that for long-span bridges, deck vibration will have a considerable impact on the efficiency of the damper to suppress cable vibration. As can be observed from Fig.4-10, compared to the conventional assumption of cable fixed at both ends, if the vibration of the bridge deck and its interaction with cable and damper supporting points are included in the formulation, for medium span length cable-stayed bridges as the Nanjing Bridge (main span 648m) and the Donghai Bridge (main span 420m), the effectiveness of the damper, in terms of the equivalent 1st modal damping ratio of the cable, has been reduced by roughly 5%. However, in the case of the Tatara Bridge, the Stonecutters Bridge and the Sutong Bridge, which has main span length of 890m, 1018m and 1088m, respectively, the impact is much more significant. For the Sutong Bridge, which has the longest main span of 1088m, the equivalent 1st modal cable damping ratio is found to be reduced by almost a half. The pattern of the current results, as shown in Fig.4-10, clearly indicates that as the main span length of the cable-stayed bridge increases, the actual performance of the damper on suppressing cable vibration will deviate more from the cable fixed-fixed case. Therefore, based on the current study, to have a more accurate estimation on the efficiency of a damper, for cable-stayed bridges with main span length exceeding 700m, the impact of deck vibration should be considered.

CHAPTER V CONCLUSIONS AND RECOMMENDATIONS

5.1 Concluding Remarks

An analytical model was proposed to determine the damping property of a bridge stay cable when attached with a damper, by considering the effect of bridge deck vibration on the cable and the damper. The proposed model comprised a bridge stay cable, an equivalent 3-span continuous beam representing the original bridge girder and all supporting cables except the one considered in the analysis, and a damper. The equation of motion of the cable and the equivalent 3-span continuous beam have been derived separately. They are coupled to yield the equation of motion of the cable-deck-damper system by applying appropriate boundary conditions at the supports and compatibility conditions at cable-deck, damper-deck and cable-damper connection points. The equivalent 1st modal damping ratio of the cable was determined by solving the system of equations. A Matlab program was developed to perform associated matrix calculation and iterations. The associated finite element model for the dynamic analysis was developed using ABAQUS 6.9.

Case studies were carried out to investigate the effect of cable-deck interaction on the damper efficiency for cable-stayed bridges with different span lengths. Five cable-stayed bridges with a main span ranging from 423m to 1088m were selected for this purpose. The validity of the model was verified by assuming a very rigid equivalent beam and compared with the results obtained from a cable fixed-fixed case. The main conclusions obtained from the current research are

- Developed a 3-span continuous beam model to study the impact of bridge- deck vibration on the efficiency of an external damper on suppressing bridge stay cable

vibration. The validity of the model was verified by theoretical approach with cable fixed-fixed support condition.

- Applied the proposed model to a long-span cable stayed bridge-Sutong Bridge (main span 1088m). Results show that by considering the vibration of the bridge-deck and its interaction with cable and damper, the efficiency of the damper has been reduced almost by 50%.
- Conducted case studies for five medium to long-span cable-stayed bridges. It was found that if the main span length of the bridge exceeds 700m, it is necessary to include deck vibration effects in damper design.

Compared to the existing models and methods, the advantages of the proposed model in evaluating damping ratio are

- The proposed model allows the cable – deck interaction to be incorporated into the analysis.
- The model uses the real configuration of bridge structure in both static and dynamic analyses leading to more accurate results.
- Higher modes of cable vibration can be analysed using the same model.
- The model results are exact, no interpolation involved in the calculation.
- The model can be used to optimize damper design for cables on long-span cable-stayed bridges.

5.2 Recommendations for Future Research

In the proposed model, the cable is assumed as a taut string of which the bending stiffness is ignored. But for more accurate results, the effect of sag and bending stiffness of the cable needs to be considered in the analysis. When dynamically excited, in addition to the cable in-plane vibration, the bridge girder can be subjected to the out- of-plane movements such as shear and torsional effects. Such effects may influence the damper efficiency as well. Therefore in future studies, these effects should also be considered in evaluating damper efficiency.

APPENDIX A

RELATIONSHIP BETWEEN m_2 AND EI IN THE EQUIVALENT BEAM BASED ON THE STATIC CONDITION

The static deflection of the equivalent beam at cable anchorage location is formulated based on two types of loads acting on the bridge girder, i.e. deflection due to the self weight of the equivalent beam and deflection due to cable tension at the anchorage point.

- a) Deflection due to self weight of the equivalent beam using the three-moment theorem.

A schematic of a continuous three-span beam with self weight of w_2 and bending stiffness EI is shown in Fig. A-1. Areas A_1, A_2, A_3 refers to the area of the bending moment diagram for given loading on each span under simply supported conditions. When using the three-moment theorem, x_1 is the distance to the centre of gravity of the bending moment diagram of span1 measured from support A and x_2 is the distance to the centre of gravity of the bending moment diagram of span 2 measured from support C. The lengths of spans AB, BC and CD are L_1, L_2 and L_3 and the bending moments at B and C are M_{B1} and M_{B2} , respectively. R_{A1}, R_{B1}, R_{C1} and R_{D1} refer to support reactions at A,B,C and D, respectively. Distances x and y are measured as shown.

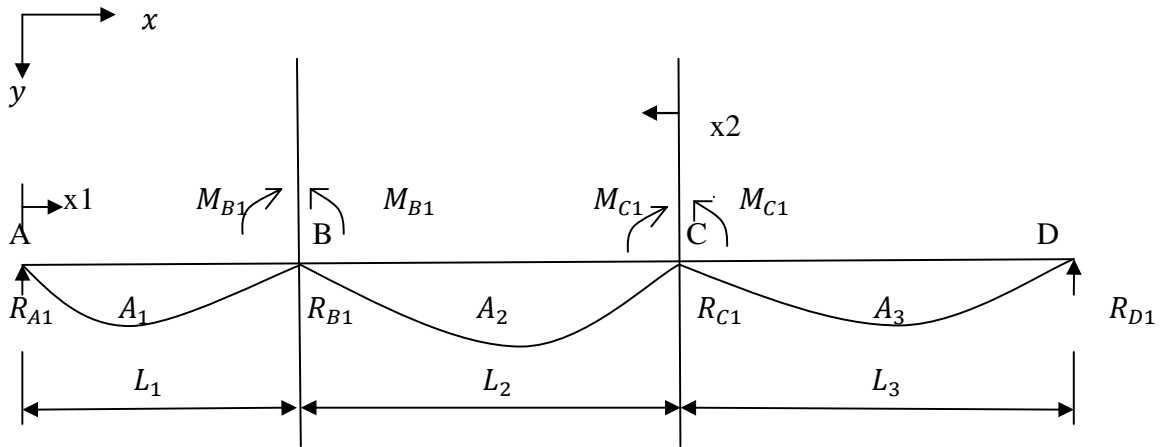


Figure A-1 Three- span continuous beam under self weight loading, including bending moment diagrams for each span in simply supported condition.

Considering equilibrium of span ABC, the three moment theorem is applied;

$$M_{A1} \frac{L_1}{I} + 2M_{B1} \left(\frac{L_1}{I} + \frac{L_2}{I} \right) + M_{C1} \frac{L_2}{I} = 6 \left(\frac{A_1}{L_1} \frac{x_1}{I} + \frac{A_2}{L_2} \frac{x_2}{I} \right) \quad (\text{A-1})$$

$$A_1 = \frac{w_2}{12} L_1^3, \quad x_1 = \frac{L_1}{2} \quad A_2 = \frac{w_2}{12} L_2^3, \quad x_2 = \frac{L_2}{2} \quad M_A = M_D = 0$$

Substituting into Eq. (A-1) gives

$$2M_{B1}(L_1 + L_2) + M_{C1}L_2 = \frac{w_2}{4} (L_1^3 + L_2^3) \quad (\text{A-2})$$

Similarly, considering span BCD

$$2M_{C1}(L_2 + L_3) + M_{B1}L_2 = \frac{w_2}{4}(L_2^3 + L_3^3) \quad (\text{A-3})$$

Shear Forces are given by;

$$R_{A1} = \frac{w_2}{2}L_1 - \frac{M_{B1}}{L_1} \quad (\text{A-4})$$

$$R_{D1} = \frac{w_2}{2}L_3 - \frac{M_{C1}}{L_3} \quad (\text{A-5})$$

$$R_{B1} = \frac{w_2}{2L_2}(L_1 + L_2)^2 - \frac{R_{A1}(L_1+L_2)}{L_2} - \frac{M_{C1}}{L_2} \quad (\text{A-6})$$

Deflection y at a distance x from the left support of the mid-span is given by;

$$y = \frac{-w_2}{24EI}x^4 + \frac{R_{B1}}{6EI}x^3 - \frac{M_{B1}}{2EI}x^2 + \left(\frac{w_2}{24EI}L_2^3 + \frac{M_{B1}}{2EI}L_2 - \frac{R_{B1}}{6EI}L_2^2 \right)x \quad (\text{A-7})$$

b) Deflection due to cable tension at the anchorage point.

A general case of deflection at location E due to a load P acting on a 3-span continuous beam ABCD shown in Figure A-2 is considered first. Span lengths of AB, BC and CD are L_1 , L_2 and L_3 . L is the distance to the load P measured from support B. M_{B2} and M_{C2} represent the bending moments at supports B and C while R_{A2} , R_{B2} , R_{C2} and R_{D2} are reactions at A, B, C and

D, respectively. Load P will be replaced by the vertical component of cable tension in upward direction afterwards.

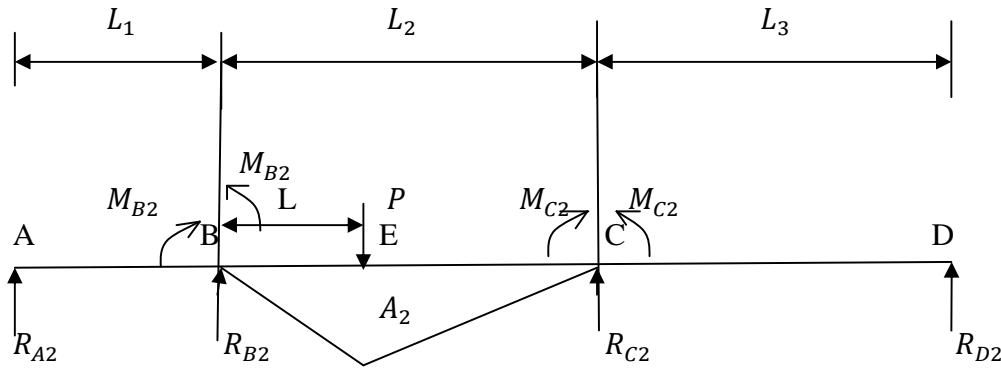


Figure A-2 Three - span continuous beam subjected to a concentrated load, including the bending moment diagram for simply supported case.

Using moments and reactions as shown in Fig. A-2

$$M_{A2} = M_{D2} = 0, \quad A_1 = A_3 = 0, \quad A_2 = \frac{PL(L_2-L)}{2}, \quad x_1 = \frac{(L_2+L)}{3}, \quad x_2 = \frac{(2L_2-L)}{3}$$

Substituting the values above into Eq. (A-1) for span ABC, we obtain;

$$2M_{B2}(L_1 + L_2) + M_{C2}L_2 = PL(L_2 - L)(2L_2 - L)/L_2 \quad (\text{A-8})$$

Substituting the values above into Eq. (A-1) for span BCD, we obtain;

$$M_{B2}L_2 + M_{C2}(L_2 + L_3) = PL(L_2 - L)(L_2 + L)/L_2 \quad (\text{A-9})$$

Shear forces are given by;

$$R_{A2} = -\frac{M_{B2}}{L_1} \quad (\text{A-10})$$

$$R_{C2} = -\frac{M_{C2}}{L_3} \quad (\text{A-11})$$

$$R_{B2} = \frac{P(L_2-L)}{L_2} - \frac{R_{A2}(L_1+L_2)}{L_2} - \frac{M_{C2}}{L_2} \quad (\text{A-12})$$

Deflection y at a distance x from the left support of the mid-span is given by;

$$y = \frac{R_{B2}}{6EI} x^3 - \frac{M_{B2}}{2EI} x^2 - P \frac{(x-L)^3}{6EI} + \left(\frac{M_{B2}}{2EI} L_2 - \frac{R_{B2}}{6EI} L_2^2 + P \frac{(L_2-L)^3}{6L_2EI} \right) x \quad (\text{A-13})$$

Since the deflection at the cable anchorage location is adjusted to zero at the time of construction, the upward deflection of the bridge deck due to cable tension at the anchorage point should be equal to the downward deflection due to self weight of the bridge at that location.

Hence, substituting $x = L$ into Eq. (A-7) gives

$$y_1 = \frac{-w_2}{24EI} L^4 + \frac{R_{B1}}{6EI} L^3 - \frac{M_{B1}}{2EI} L^2 + \left(\frac{w_2}{24EI} L_2^3 + \frac{M_{B1}}{2EI} L_2 - \frac{R_{B1}}{6EI} L_2^2 \right) L \quad (\text{A-14})$$

Substituting $P = -T \sin \theta$ and $x = L$ into Eq. (A-13) gives

$$y_2 = \frac{R_{B2}}{6EI} L^3 - \frac{M_{B2}}{2EI} L^2 + \left(\frac{M_{B2}}{2EI} L_2 - \frac{R_{B2}}{6EI} L_2^2 + P \frac{(L_2-L)^3}{6L_2EI} \right) L \quad (\text{A-15})$$

The condition for zero deflection is;

$$y_1 + y_2 = 0 \quad (\text{A-16})$$

APPENDIX B

RELATIONSHIP OF m_2 AND EI IN THE EQUIVALENT BEAM BASED ON THE FIRST VERTICAL BENDING FREQUENCY OF THE BRIDGE

A two-dimensional finite element model of a cable-deck system was developed using the general purpose finite element software ABAQUS. Both the cable and the deck were represented by B21 two-node linear in-plane beam elements. The cable tension under static loading was represented by an initial stress in the cable. The finite element model is schematically shown in Fig. B-1.

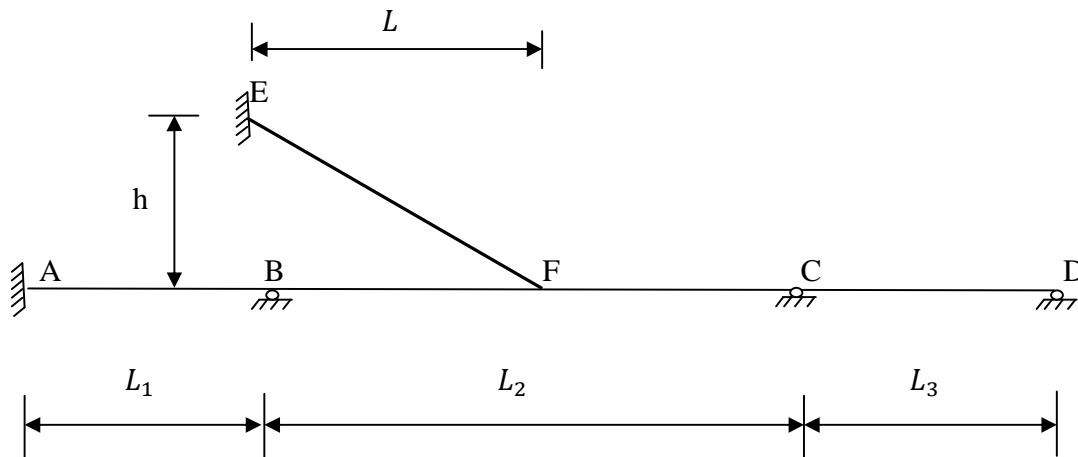


Figure B-1 schematic diagram of the numerical model of cable-deck system

In Fig. B-1, ABCD represents the equivalent bridge girder, support A has restricted movements in both horizontal and vertical directions whereas supports B, C and D only have restricted vertical movements. EF represents the cable under investigation. Support E is a fixed support and support F is free to move. Young's modulus for steel and the given section of the

cable was used as the cable properties. For the bridge girder, a hollow rectangular section was used with element type B21 and Young's modulus for concrete was used and the density of the material was varied to satisfy the deflection criterion while satisfying the frequency requirement. The analysis was performed in two steps. step1 as the static general case and step2 as the linear perturbation, frequency. The Lanczos eigen solver was selected as the method and requested for 20 eigen values.

To get an idea about the number of elements required for accurate solution of vibration frequency, ABAQUS simulation was conducted for the beam ABCD by using different mesh sizes. The span lengths used were $L_1 = 300m$, $L_2 = 1088m$ and $L_3 = 300m$. It was found that an element length of 10m or less gives an accurate solution up to the third decimal place of the frequency value. Hence an element size of 10m was considered optimum to mesh the beam. Since the cable length was 577m and it was also meshed using the B21 beam element, the same optimum mesh size is applicable for the cable.

Since the mass density of the bridge girder is unknown at the beginning, a bridge girder section has to be assumed initially and the frequency value of the cable-deck system must be verified. This will be a trial and error procedure until the frequency value is obtained and the static displacement at the cable anchorage point is zero.

APPENDIX C

**MODEL DAMPING RATIO OF AN INCLINED TAUT STRING WITH FIXED
SUPPORTS ATTACHED TO A LINEAR VISCOUS DAMPER**

Fig. C-1 shows a cable-damper system comprised of an inclined cable connected to fixed supports at A and B and a damper, connected to the cable at C and connected to a fixed support at D.

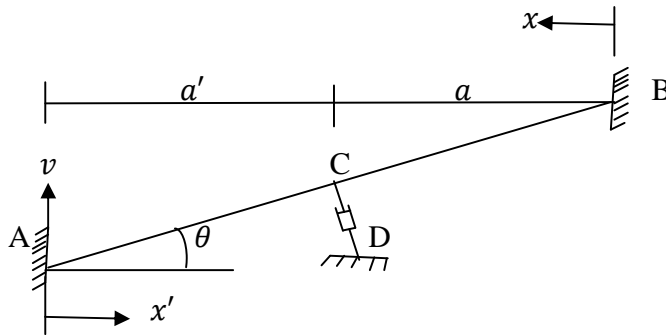


Figure C-1 A cable-damper system

The following equation can be obtained considering the in-plane vertical motion of the inclined cable AB of the cable-damper system.

$$\frac{H}{\sqrt{1+\left(\frac{dy}{dx}\right)^2}} \frac{\partial^2 v}{\partial x^2} = \rho \frac{\partial^2 v}{\partial t^2} \quad (\text{C-1})$$

where H is the horizontal component of the cable tension T , $y(x)$ is the static profile of the cable, ρ is the mass density of the cable, $v(x,t)$ is the vertical in-plane dynamic displacement of the cable with respect to time t and the other dimensional parameters are as shown in the Fig.C-1.

$$H = T \cos \theta \quad (\text{C-2})$$

If the sag in the cable is neglected;

$$\frac{dy}{dx} = \tan \theta \quad (\text{C-3})$$

Substituting Eq.(C-3) into Eq.(C-1) and rewriting, considering the damper force F_v at $x = a$; we obtain:

$$T \cos^2 \theta \frac{\partial^2 v}{\partial x^2} - \rho \frac{\partial^2 v}{\partial t^2} = -F_v \delta(x - a) \quad (\text{C-4})$$

Where δ is the Dirac delta function.

Damping force at $x = a$ can be expressed as;

$$T \cos \theta \left\{ \left. \frac{dv}{dx} \right|_{a^+} - \left. \frac{dv}{dx} \right|_{a^-} \right\} = -F_v \quad (\text{C-5})$$

Also

$$-F_v = C \frac{dv(a,t)}{dx} \quad (\text{C-6})$$

where C is the damper capacity.

Assuming

$$v(x,t) = v_1(x)e^{i\omega t} \quad 0 \leq x < a \quad (\text{C-7})$$

$$v(x,t) = v_2(x')e^{i\omega t} \quad 0 \leq x' < a' \quad (\text{C-8})$$

Also assuming

$$v_1(x) = A_1 \sin(\gamma x) + B_1 \cos(\gamma x) \quad (\text{C-9})$$

$$v_2(x) = A_2 \sin(\gamma x') + B_2 \cos(\gamma x') \quad (\text{C-10})$$

The boundary conditions are:

$$v(0,t) = 0 \rightarrow v_1(0) = 0 \rightarrow v_1(x) = A_1 \sin(\gamma x) \quad (\text{C-11})$$

$$v(L,t) = 0 \rightarrow v_2(0) = 0 \rightarrow v_2(x') = A_2 \sin(\gamma x') \quad (\text{C-12})$$

where $\gamma = \frac{\omega}{\cos\theta} \sqrt{\frac{m}{T}}$

Substituting Eqs.(C-11),(C-12) and (C-6) into Eq.(C-5)

$$A_1(\cos(\gamma a) + i\beta \sin(\gamma a)) + A_2 \cos(\gamma a') = 0 \quad (\text{C-13})$$

where $\beta = \frac{c\omega}{\gamma T \cos\theta}$

The continuity condition at C ;

$$v_1(a)e^{i\omega t} = v_2(a')e^{i\omega t} \rightarrow A_1 \sin(\gamma a) = A_2 \sin(\gamma a') \quad (\text{C-14})$$

Substituting Eq.(14) into Eq.(13) ;

$$A_1(\cos(\gamma a) + i\beta \sin(\gamma a)) + A_1 \sin(\gamma a) \cot(\gamma a') = 0 \quad (\text{C-15})$$

Since $A_1 \neq 0$; Eq.(C-15) yields the transcendental equation for the cable motion as

$$(\cos(\gamma a) + i\beta \sin(\gamma a)) + \sin(\gamma a) \cot(\gamma a') = 0 \quad (\text{C-16})$$

The solution of Eq.(C-16), γ , yields the complex frequency ω , from which the damping ratio ξ can be determined.

APPENDIX D MATLAB PROGRAM FOR MATRIX CALCULATIONS AND ITERATIONS

D-1 Matlab program to calculate eigen frequencies of cable-damper-deck system

```

%Model analysis of Sutong Bridge
%This program calculates the eigen frequencies of the model
clear,clc
theta=0.392;      %Angle of inclination of the cable
x=0.0127;      %This is the damper location parameter;x=Ld/L
Lc=577;      %Length of the cable
L=Lc*cos(theta); %Horizontal distance from the cable anchorage point to the
pylon
Ld=x*Lc;      %Distance along the cable to the damper connection
a1= Ld*cos(theta);
b1=Ld/cos(theta);
a=L-a1;b=L-b1;
m1= 100.8; % Mass density of the cable kg/m
m2= 264.971; % Mass density of the equivalent bridge girder kg/m
C0= 325000; % Damping capacity of the damper N.s/m
L1= 300; %Length of span 1
L2=1088; %Length of main span
L3= 300; %Length of span 3
L4= L2-L;
T=6708000; %Cable tension under static condition N
EI=3.11E11; %Bending stiffness of the equivalent bridge girder N.m^2
syms w
ga=w/cos(theta)*(m1/T)^0.5; %Parameter  $\gamma$ 
be=C0*w/ga/T/cos(theta); %Parameter  $\beta$ 
la=(m2/EI)^0.25*w^0.5; %Parameter  $\lambda$ 
ne=C0*w/la^3/EI; %Parameter  $\eta$ 

D=[cos(la*L1)-cosh(la*L1)*sin(la*L1)/sinh(la*L1) -1 0 0 0 0 -1 0 0
0 0 0;
sin(la*L1)*(cos(la*b)-cosh(la*b)) sin(la*b) 0 0 0 -1 sinh(la*b) 0 0
-1 0 0;
-sin(la*L1)*(sin(la*b)+sinh(la*b)) cos(la*b) -1 0 0 0 cosh(la*b) -
1 0 0 0 0;
-sin(la*L1)*(cos(la*b)+cosh(la*b)) -sin(la*b) 0 0 0 1 sinh(la*b) 0
0 -1 0 0;
sin(la*L1)*(sinh(la*b)-sin(la*b)+i*ne*(cos(la*b)-cosh(la*b)))
cos(la*b)+i*ne*sin(la*b) -1 0 0 0 i*ne*sinh(la*b)-cosh(la*b) 1 0 0 -
i*ne*sin(ga*a) 0;
0 0 sin(la*b1) -sin(la*L4) -sin(la*L3)*(cos(la*L4)-cosh(la*L4))
cos(la*b1) 0 sinh(la*b1) -sinh(la*L4) cosh(la*b1) 0 0;
0 0 cos(la*b1) cos(la*L4) -sin(la*L3)*(sin(la*L4)+sinh(la*L4)) -
sin(la*b1) 0 cosh(la*b1) cosh(la*L4) sinh(la*b1) 0 0;
0 0 -sin(la*b1) sin(la*L4) sin(la*L3)*(cos(la*L4)+cosh(la*L4)) -
cos(la*b1) 0 sinh(la*b1) -sinh(la*L4) cosh(la*b1) 0 0;
0 0 -cos(la*b1) -cos(la*L4) sin(la*L3)*(sin(la*L4)-sinh(la*L4))
sin(la*b1) 0 cosh(la*b1) cosh(la*L4) sinh(la*b1) 0
ga*T*cos(theta)/la^3/EI;

```

```

0 0 0 1 -cos(la*L3)+sin(la*L3)*cosh(la*L3)/sinh(la*L3) 0 0 0 1
0 0 0;
0 0 sin(la*b1) 0 0 cos(la*b1) 0 sinh(la*b1) 0 cosh(la*b1) -
sin(ga*a)/cos(ga*a1) tan(ga*a1);
0 0 0 0 0 i*be 0 0 0 i*be -cos(ga*a)-
i*be*sin(ga*a)+tan(ga*a1)*sin(ga*a) -cos(ga*a1)-tan(ga*a1)*sin(ga*a1)];

k1=1;
for k1=1:12
    k2=1;
    for k2=1:12
        F=D(k1,k2);
        F1=diff(F,'w');
        E(k1,k2)=subs(F,[w],[1.405])+subs(F1,[w],[1.405])*(w-1.405);
    end
end
S=det(E)
S1=solve(S);S2=S1(:,1)

```

D-2 Model analysis for fixed inclined cable-damper system

```

%This programm calculates the eigen frequencies of the model
clear,clc
theta=0.392; %Angle of inclination of the cable
x=0.0127; %This is the damper location parameter;x=Ld/L
Lc=577; %Length of the cable
L=Lc*cos(theta); %Horizontal distance from the cable anchorage point to the
pylon
Ld=x*Lc; %Distance along the cable to the damper connection
a1= Ld*cos(theta);
b1=Ld/cos(theta);
a=L-a1;b=L-b1;
m1= 100.8; % Mass density of the cable kg/m
m2= 264.971; % Mass density of the equivalent bridge girder kg/m (not
used)
C0= 325000; % Damping capacity of the damper N.s/m
L1= 300; %Length of span 1
L2=1088; %Length of main span
L3= 300; %Length of span 3
L4= L2-L;
T=6708000; %Cable tension under static condition N
EI=3.11E11; %Bending stiffness of the equivalent bridge girder N.m^2(not
used)
syms w
ga=w/cos(theta)*(m1/T)^0.5;%Parameter  $\gamma$ 
be=C0*w/ga/T/cos(theta);%Parameter  $\beta$ 
la=(m2/EI)^0.25*w^0.5;%Parameter  $\lambda$ 
ne=C0*w/la^3/EI;%Parameter  $\eta$ 

D=[cos(ga*a) sin(ga*a) cot(ga*a1)];
for k=1:3
    F=D(k);
    F1=diff(F);

```



```
E(k)=subs(F,[w],[1.369])+subs(F1,[w],[1.369])*(w-1.369);  
end  
EQ=E(1)+be*i*E(2)+E(2)*E(3);  
A=solve(EQ)
```

APPENDIX E INPUT SOURCE CODE FOR ABAQUS SIMULATION

**FREE VIBRATION SIMULATION OF CABLE-DECK SYSTEM OF SUTONG

BRIDGE

** Job name: Job-1 Model name: SUTONG

** Generated by: Abaqus/CAE 6.9-1

*Preprint, echo=NO, model=NO, history=NO, contact=NO

**DEFINE NODES AT SUPPORTS AND LOCATIONS OF CHANGE IN PROPERTIES

*Node

1,0,0

21,300,0

56,824.9795,0

57,832.924,0

94,1388,0

114,1688,0

115,300,220.308

154,826.139,2.8043

**GENERATE NODES IN BETWEEN KNOWN NODES

*NGEN,NSET=B

1,21,1

21,56,1

57,94,1

94,114,1

*NGEN,NSET=C

115,154,1

**DEFINE ELEMENTS

*Element, type=B21

1, 1, 2

21, 21, 22

56, 56, 57

57, 57, 58

94, 94, 95

115, 115, 116

154, 154, 57

**GENERATE ELEMENTS USING ALREADY DEFINED ELEMENTS

*ELGEN,ELSET=BEAM1

1,20,1,1

21,35,1,1

57,37,1,1

94,20,1,1

**NAME ELEMENT SETS

*ELSET, ELSET=BEAM

BEAM1

56,

```

*ELGEN,ELSET=CABLE1
115,39,1,1
*ELSET,ELSET=CABLE
CABLE1,
154,
**NAME NODE SETS
*Nset, nset=N154
154,
*Nset, nset=N56
56,
** DEFINE CABLE SECTION
*Beam Section, elset=CABLE, material=STEEL, temperature=GRADIENTS, section=CIRC
0.065
0.,0.,-1.
** DEFINE BEAM SECTION
*Beam Section, elset=BEAM, material=CONCRETE, temperature=GRADIENTS, section=BOX
36., 5.55, 0.18, 0.18, 0.18, 0.18
0.,0.,-1.
**DEFINE LOCATION OF DAMPER
*Element, type=DashpotA, elset=dashpot1
251, 154, 56
**DEFINE DAMPER CAPACITY
*Dashpot, elset=dashpot1

325000.
** DEFINE NODE SETS
*Nset, nset=N1
1,
*Nset, nset=NSS
21,
94,
114,
*Nset, nset=N57
57,
*Nset, nset=N115
115,
**End Assembly
**DEFINE INITIAL STRESS ;REF.INITIAL TENSION
*INITIAL CONDITIONS,TYPE=STRESS
CABLE,5.05E8,0,0.
**
** MATERIALS
** DEFINE MATERIAL PROPERTIES
*Material, name=CONCRETE
*Density
15.2,

```

```

*Elastic
3e+9, 0.15
*Material, name=STEEL
*Density
7850.,
*Elastic
2e+11, 0.3
** -----
**STEP1 STATIC
*Step, name=Step-1, nlgeom=YES
*Static
1., 6., 1e-05, 6.
**DEFINE BOUNDARY CONDITIONS
** BOUNDARY CONDITIONS
**
*Boundary
N1, 1, 1
*Boundary
N1, 2, 2
*Boundary
NSS, 2, 2
*Boundary
N115, 1, 1
*Boundary
N115, 2, 2
**
** OUTPUT REQUESTS
**
**Loads; Type:Gravity
**Dload
**BEAM, GRAV, 9.81, 0., -1.
**CABLE, GRAV, 9.81, 0., -1.
**
**
**
*Restart, write, frequency=0
**
** FIELD OUTPUT: F-Output-1
*Output, field, variable=PRESELECT
*Output, history, variable=PRESELECT
*End Step
** -----
**DEFINE STEP 2 LINEAR PERTURBATION
** STEP: Step-2
**
*Step, name=Step-2, perturbation

```

```
frequency
*Frequency, eigensolver=Lanczos, acoustic coupling=on, normalization=displacement
20, , , ,
**
*Restart, write, frequency=0
**
*Output, field, variable=PRESELECT
*End Step
```

REFERENCES

1. Bosdogianni, A., Olivari, D. (1996), Wind- and rain- induced oscillations of cables of stayed bridges. *Journal of Wind Engineering and Industrial Aerodynamics*, Vol. 64, 171-185
2. Carrion-Viramontes, F. J., Lopez, J.A. , Quintana-Rodriguez, J.A., Lozano-Guzman A., (2008). Nonlinear Assessment of Cable Vibration in a Stayed Bridge., *Experimental Mechanics* 48: 153-161.
3. Caetano,Elsa de Sa.(2006). Cable Vibrations in Cable-Stayed Bridges. *International Association for Bridge and Structural Engineering*.
4. Cheng S.H., David T. Lau.,(2002). Modeling of cable vibration effects of cable-stayed bridges. *Earthquake Engineering and Engineering Vibration*, Vol.1 No.1:74-85.
5. Cheng, S., Deravandi, N. and Ghrib, F. (2010), “Identification of structural damping in a stay cable with transverse viscous damper using energy-based approach”, *Journal of Sound and Vibration, In Press*
6. Cheng, S. and Koralalage, K. (2009), “Prediction of modal damping of a cable-damper system using energy-based approach”, *Proceeding of 8th International Symposium on Cable Dynamics*, Paris, France, pp.293-300
7. Cheng, S., Tanaka, H. (2002), “Cable Aerodynamics: The state-of-the-art”, *The 2nd International Symposium on Advances in Wind and Structures*, Pusan, Korea, Aug.21-23, pp.343-352
8. Douglas Thorby. (2008). *Structural Dynamics and Vibration in Practice*. Oxford,U.K., Miami,U.S.A: Elsevier Ltd.

9. Gorman Daniel J., (1975). Free Vibration Analysis of Beams and Shafts. USA:John Wiley and Sons, Inc.
10. Hikami, Y., Shiraishi, N. (1988). Rain-wind induced vibrations of cables in cable-stayed bridges. *Journal of Wind Engineering and Industrial Aerodynamics*, Vol. 29, 409-418
11. Holmes John D.,(2007) “*Wind Loading of Structures*”, London and Newyork., Taylor & Francis group
12. Irvine H.M, (1974). Dynamics, *Lab.Report DYNL-108*
13. Irvine H.M., Caughey T.K.,(1974). The linear theory of free vibrations of a suspended cable. *Proceedings of the Royal Society of London. Series A. Mathematical and Physical Sciences*, Vol.341.No.1626, 299-315.
14. Irvine Max, (1980). Cable Structures. New York: Dover Publications,Inc.
15. Kong, J. Cheung, Y. K., (1996). Vibration of continuous beams using modified beam vibration functions. *Communications in numerical methods in Engineering*, Vol.12, 107-114.
16. Koralalage, K. and Cheng, S. (2009), “Damping estimation curves for the vibration control design of bridge stay cables”, *Proceeding of 8th International Symposium on Cable Dynamics*, Paris, France, pp.301-308.
17. Kovacs, I.,(1982), Zur frage der seil-schwingungen und der seildamfung, *Bautechnik* 10, 325-332.
18. Krenk, S. (2000). Vibrations of a Taut Cable with an External Damper. *Journal of Applied Mechanics*, Vol. 67,772-776.

19. Liang Dong, Sun Li-min, Cheng Wei, (2008). Effect of girder vibration on performance of cable damper for cable-stayed bridge. *Journal of Engineering Mechanics*, Vol.25 No.5,110-116
20. Limin Sun, Chen Shi, Haijun Zhou, Wei Cheng.,(2004). A Full-scale Experiment on Vibration Mitigation of Stay Cable. *IABSE Conferences* ,Shanghai, China.
21. Macdonald John H.G.,(2004) Dynamic cable – deck interaction of cable-stayed bridges
22. Main, J.A. and Jone, N.P. (1999), Full-scale measurements of stay cable vibration. *Wind Engineering into the 21st Century*, Larsen, Larose & Livesey (eds), Balkema, Rotterdam, 963-970
23. Main, J.A., Jone, N.P., Yamaguchi, H. (2001), Characterization of rain-wind induced stay-cable vibrations from full-scale measurements. *Proceedings of 4th International Symposium on Cable Aerodynamics*, Montreal, 235-242
24. Main J.A., Jones N.P., (2002). Free vibrations of Taut cable with attached damper. I: Linear Viscous Damper. *Journal of Engineering Mechanics*:1062-1071.
25. Main J.A., Jones N.P., (2002). Free vibrations of Taut cable with attached damper. II: Nonlinear Viscous Damper. *Journal of Engineering Mechanics*:1072-1081.
26. Marcin Maslanka, (2007). Free vibrations of a cable with an attached MR damper- experimental analysis of amplitude dependent damping. *Proceedings of the 7th International Symposium on Cable Dynamics*. 415-422.
27. Masahiro Yoneda, Ken-ich Maeda,. A study on practical estimation method for structural damping of stay cable with dampers.

28. Matsumoto, M., Yokoyama, K., Miyata, T., Fujino, Y. and Yamaguchi, H. (1989b), Wind-induced cable vibration of cable-stayed bridges in Japan. Proceeding of *Canada-Japan Workshop on Bridge Aerodynamics*, Ottawa, Canada, September 25-27, 101-110
29. Matsumoto, M., Shiraishi, N., Kitazawa, M., Knisely, C., Shirato, H., Kim, Y, Tsujii, M.(1990), Aerodynamic behaviour of inclined circular cylinders-cable aerodynamics. *Journal of Wind Engineering and Industrial Aerodynamics*, Vol. 33, 63-72
30. Mehrabi Armin B. ,Tabatabai Habib.,(1998). Unified finite difference formulation for free vibration of cables. *Journal of Structural Engineering*:1313-1322.
31. Pacheco,B.M., Fujino,Y., Sulekh, A.(1993). Estimation curve for modal damping in stay cables with viscous damper. *Journal of Structural Engineering ASCE* 119(6), 1961-1979.
32. Peng Wei, Sun Bingnan, Tang Jinchun, (1999). A catenary element for the analysis of cable structures. *Applied Mathematics and Mechanics*, Vol.2 No.5, 532-534.
33. Rao V. Dukkupati, Sirinivas,J., (2007). *Vibrations-Problem Solving Companion*. Oxford, U.K.: Alpha Science International Ltd.
34. Saito, T., Matsumoto, M., Kitazawa, M. (1994), Rain-wind excitation of cables on cable-stayed Higashi-Kobe Bridge and cable vibration control. *Proceedings of the International Conference on Cable-stayed and Suspension Bridges (AFPC)*, Deauville, Vol. 2, 507-514
35. Singiresu Rao S.,(2007). *Vibration of continuous systems*. New Jersey: John Wiley & Sons,Inc.
36. Starossek, U.,(1994). Cable Dynamics-A Review. *Structural Engineering International*, 3/94,171-176.
37. Strouhal, V. (1898), Uber eine besondere Art der Tonerregung. *Annl. Phys.*, Vol. 5

38. Sun Bing-nan, Wang Zhi-gang, Ko,J.M. Ni,Y.Q. (2003). Parametrically excited oscillation of stay cable and its control in cable-stayed bridges, *Journal of Zhejiang University Science* V.4. No.1,13-20.
39. Tabatabai Habib & Mehrabi Armin B.,(2000).Design of Mechanical Viscous Dampers for Stay Cables. *Journal of Bridge Engineering*:114-123.
40. Triantafyllou,M.S., (1983). The dynamics of taut inclined cables. *Journal of Mechanics and Applied Mathematics*, Vol.37,421-440.
41. Uno,K.,Kitagawa,S.,Tsutsumi,J.,Inoue,A. and Nakaya,S. (1991). A simple method of designing cable vibration dampers of cable- stayed bridges. *Journal of Structural Engineering*, Toyko, 37A.789-798.
42. Virlogeux, M. (1998), Cable vibrations in cable-stayed bridges. *Bridge Aerodynamics*, Larsen & Esdahl (eds), Balkema, Rotterdam, 213-233
43. Vejrum, T., Carter, M. & Kite, S. (2006), “Detailed Design of Stonecutters Bridge Superstructure”, Proceedings of International Conference on Bridge Engineering – Challenges in the 21st Century, Hong Kong.
44. Wang Lingyun, Xu Y.L.,(2003). *Wind-rain-induced vibration of cable: an analytical model(1)*. International Journal of Solids and Structures 40:1265-1280.
45. Wardlaw, R.L., Cooper, K.R. and Scanlan, R.H. (1973), Observations on the problem of subspan oscillation of bundled power conductors. DME/NAE Quarterly Bulletin No.(1)
46. Wu, Q. Takahashi, K. Nakamura, S.(2005). Formulae for frequencies and modes of in-plane vibrations of small-sag inclined cables. *Journal of Sound and Vibration*, 279(2005) 1155-1169.

47. Xu Y.L., Zhou H.J.,(2007). Damping cable vibration for a cable-stayed bridge using adjustable fluid dampers. *Journal of Sound and Vibration*:349-360.
48. Xu,Y.L., Yu, Z. (1999). Non-linear vibration of cable-damper systems partII: Application and Verification. *Journal of Sound and Vibration*(1999)225(3),465-481.
49. Yabuno M., Fujiwara T., Sumi K., Nose T., and Suzuki M.(2003). Design of “Tatara Bridge”. *IHI Engineering Review* vol.36 No.2 June 2003.
50. Yamada, H. (1997), Control of wind-induced cable vibrations from a viewpoint of the wind resistance design of cable-stayed bridges. *Proceedings of the 2nd International Seminar on Cable Dynamics*, Tokyo, 129-138
51. Yamaguchi, H & Nagahawatta, H.D.(1995). Damping effects of cable cross-ties in cable-stayed bridges. *Journal of Wind Engineering and Industry Aerodynamics*,54/55,pp35-43
52. Yoneda, M., Maeda, K.,(1989). A study on practical estimation method for structural damping of stay cable with damper. *Proceeding of Canada-Japan Workshop on Bridge Aerodynamics*. 119-128.
53. Yoshimura, T., Inoue, A., Kaji, K. and Savage, M.G. (1989), A study on the aerodynamic stability of the Aratsu Bridge. *Proceedings of Japan-Canada Joint Workshop on Bridge Aerodynamics*, 41-50
54. Yusuf Yesilce, Oktay Demirdag, Seval Catal., (2008). Free vibrations of a multi-span Timoshenko beam carrying multiple spring-mass systems. *Sadhana* Vol.33, part 4, 385-401.
55. Zhu L.D., Wang M., Wang D.L., Guo Z.S., Cao F.C.,(2007). Flutter and buffeting performances of Third Nanjing Bridge over Yangtze River under yaw wind via

aeroelastic model test. *Journal of Wind Engineering and Industrial Aerodynamics* 95: 1579-1606.

VITA AUCTORIS

NAME : Krishanth Gamini Ambagaha Koralalage

PLACE OF BIRTH : SriLanka

EDUCATION : University of Moratuwa, SriLanka
1986-1991. BSc.(Eng) Hons.
University of Windsor, Windsor, Ontario, Canada
2007-2009 MEng.
University of Windsor, Windsor, Ontario, Canada
2009-2011 MAsc.